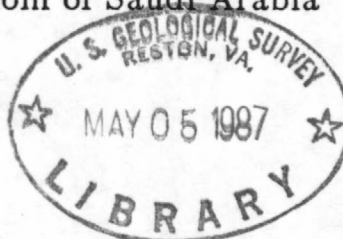# DEPARTMENT OF THE INTERIOR
U.S. GEOLOGICAL SURVEY

Probabilistic estimates of the seismic ground motion hazard in
western Saudi Arabia, Kingdom of Saudi Arabia

by

P. C. Thenhaus, S. T. Algermissen, D. M. Perkins,
S. L. Hanson, and W. H. Diment

Open-File Report 87-173

Report prepared by the U.S. Geological Survey in cooperation with the
Deputy Ministry for Mineral Resources, Saudi Arabia

This report is preliminary and has not been reviewed for conformity
with U.S. Geological Survey editorial standards and stratigraphic nomenclature.

1987

CONTENTS

ILLUSTRATIONS

TABLES

PROBABILISTIC ESTIMATES OF THE SEISMIC GROUND MOTION HAZARD IN WESTERN SAUDI ARABIA

by

Paul C. Thenhaus[1], S. T. Algermissen[1], David M. Perkins[1],
Stanley L. Hanson[1], and William H. Diment[1]

ABSTRACT

Estimates of seismic horizontal ground acceleration and velocity having a 90-percent probability of nonexceedance in 100 yrs in western Saudi Arabia indicate the highest relative levels of ground motion are expected in regions neighboring the Gulf of Aqaba and North Yemen. Estimated ground motions within the shield area are relatively low while the central and northern coastal plain regions are characterized by intermediate-level ground motion values that are generally governed by far-field effects of earthquakes in the central Red Sea rift.

The seismic hazard estimates are derived from regional seismic source zones that are based on interpretations and assumptions relating potential seismic activity to the Precambrian through Tertiary structural framework of the region. Because statistical variability in ground motion attenuation relations is known to be a dominant source of uncertainty in estimated probabilistic ground motion values, and because strong-motion records do not exist for the Arabian peninsula, hazard maps have been developed using both a preferred low-Q attenuation function and a conservative high-Q attenuation function. Values resulting from the high-Q attenuation function are considered upper bound estimates to the hazard model.

Progress toward a more complete understanding of the seismic hazards of western Saudi Arabia will come from a broad scope, interdisciplinary geological, seismological, and related geophysical investigations aimed at improving our understanding of all parameters that have gone into the probabilistic ground-motion estimates. Identification of areas in which geological hazards such as landsliding and liquefaction may occur for ground shaking levels suggested in this report will do much to quantify these hazards in a preliminary manner.

INTRODUCTION

The use of probabilistic ground-motion maps to represent seismic hazard has evolved from experience with a number of other types of map representations during the 30-yr history of regional seismic hazard mapping in the United States. Historical seismicity maps are factual and can serve to warn that earthquakes occur more widely than people usually recognize. Epicenter maps, however, only provide information about the geographical location of earthquakes and occasionally, information about the depth of earthquakes. Epicenter maps provide no direct information concerning: (1) expected levels of ground motion, and (2) the generalization of historical seismicity to likely areas of future seismicity. Historic maximum intensity maps provide information on levels of

[1]U.S. Geological Survey
Denver, Colorado

damaging ground motion, but they do not provide information on the relative frequency of occurrence of specific levels of ground motion in various geographical areas. Intensity maps may, therefore, overstate the hazard in areas where a large earthquake occurred historically but where the frequency of such occurrences is low. Probabilistic seismic ground motion maps properly focus on hazardous ground motions, allow the use of interdisciplinary geological, seismological, and geophysical information to assist in the generalization of the historic record to likely areas of future earthquakes, and properly represent the hazard with respect to the expected frequency of earthquake and ground motion occurrence. Such maps of the contiguous United States (Algermissen and Perkins, 1976; Algermissen and others, 1982) have found widespread use in building code applications, regional land-use planning, emergency preparedness, and insurance analyses. In addition, such maps can serve to prioritize regions for further research and point out those studies most useful in furthering the understanding of the seismic hazard problem.

OVERVIEW OF THE PROBABILISTIC MODEL

HAZARD MODEL

In this study, earthquakes are exponentially distributed with regard to magnitude and randomly distributed with regard to time. The exponential magnitude distribution is an assumption based on empirical observation. The distribution of earthquakes in time is assumed to be Poissonian. The assumption of a Poisson process for earthquakes in time is consistent with historical earthquake occurrence insofar as it affects the regional probabilistic hazard calculation. On a regional basis, large shocks closely approximate a Poisson process, while small shocks may depart significantly from a Poisson process. The ground motions associated with small earthquakes are of only marginal interest in engineering applications and consequently the Poisson assumption serves as a useful and simple model (Cornell, 1968).

The production of a probabilistic ground motion hazard map involves the development of four constituent models. These are: (1) a seismic source model that serves to define the spatial distribution of earthquakes within the region of concern (fig. 1-A); (2) an occurrence model of earthquakes that describes the recurrence of events in time within the seismic source zones (fig. 1-B); (3) a ground-motion attenuation model which is a mathematical description of the manner in which earthquake ground motions decrease with distance from an earthquake source for various magnitude levels (fig 1-C); and (4) a probability model for calculating the expected maximum amplitude of ground motion within a given period of time corresponding to a chosen probability level for a number of individual sites in the region (fig. 1-D).

SEISMIC SOURCE ZONE MODEL

Three idealized seismic source areas are shown in figure 1-A. Earthquakes within each source zone can be modeled as: (1) point sources in areas (used to represent earthquakes for which the fault rupture lengths are small compared with the map scale being used); (2) finite rupture lengths along two dimensional (linear) fault sources; or (3) as a mixed source, for example, point sources for small earthquakes and fault (two dimensional) sources for larger earthquakes.

2
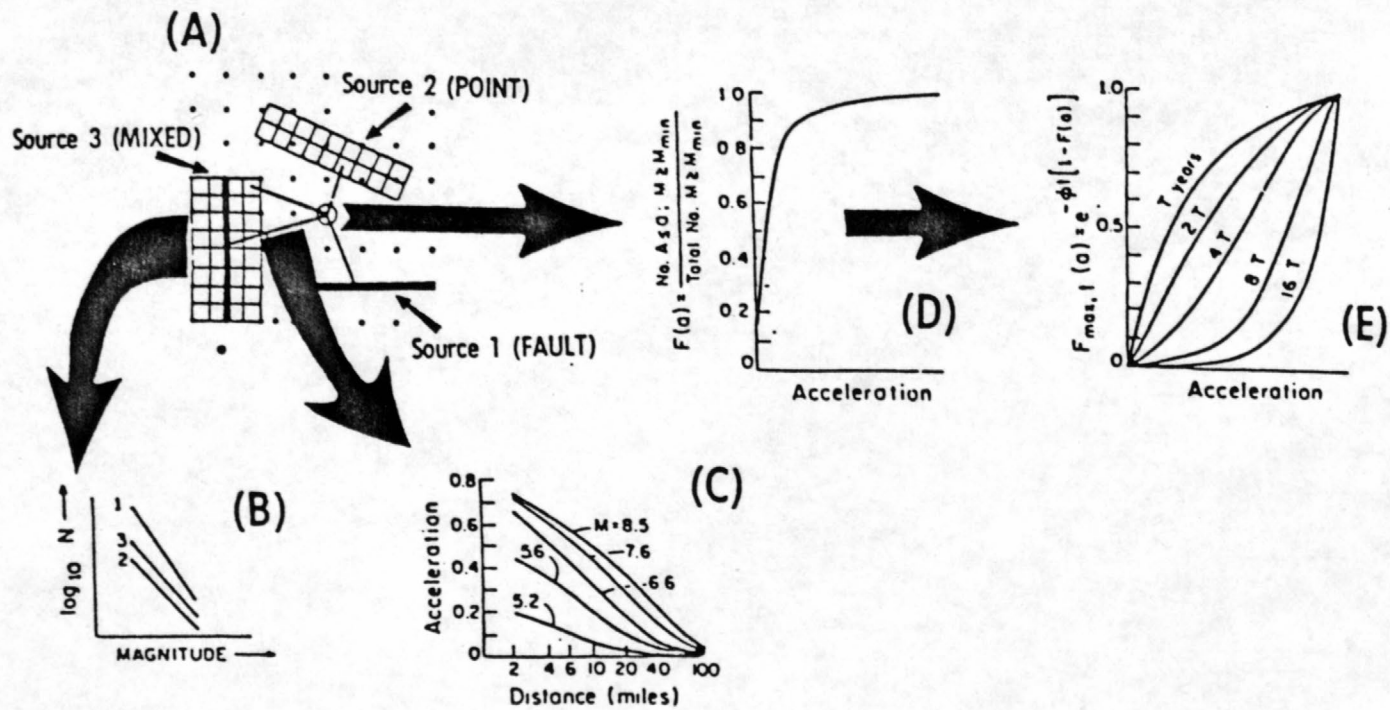
Figure 1.--*Elements of the probabilistic hazard model. A, types of seismic source zones and grid of points at which the hazard is to be computed. B, statistical analysis of seismicity data. C, ground-motion attenuation curves for various magnitude levels. D, cumulative conditional probability distribution of acceleration at a site on the grid of points. E, the extreme probability $F_{max,t}(a)$ for various accelerations and exposure times (T).*

Earthquakes are all assumed to be shallow shocks consistent with the worldwide observations of earthquake depths in regions of crustal rifting and consistent with the earthquake data base used in the development of the attenuation models applied in this study.

EARTHQUAKE OCCURRENCE MODEL

The distribution of earthquakes in time is assumed to be Poissonian (see fig. 1-B). For each seismic source, the magnitude distribution was taken to be exponential and of the form given by the Richter relation of occurrence frequencies:

$$\log N = a - bM \tag{1}$$

where N is the number of earthquakes in a given magnitude range centered about M and a and b are constants to be determined. Because seismicity in our region of concern is generally low, and research has shown that significant errors in the computed b-value occur when the total number of earthquakes are less than about 40 (Bender, 1982), b-values for regional collections of source zones having total numbers of earthquakes from 60 to 150 were computed. The b-values were computed using maximum likelihood techniques described by Bender (1983) and Weichert (1980).

The small number of earthquakes in many of the seismic source zones also precludes direct assessment of a-values for individual zones. Hence, a regional rate of earthquake activity was calculated by summing all of the activity in all of the seismic source zones. This regional rate of activity was then apportioned among the individual source zones so that the amount of activity applied to any one zone is in rough proportion to the number of earthquake events occurring in that zone. The procedure, therefore, attempts to maintain the relative seismic flux among source zones consistent with the historic record of events up to some maximum magnitude assigned to each zone.

The future spatial occurrence of earthquakes is assumed to be uniform throughout each source zone. That is, if each seismic source area is divided into n small divisions (such as shown in fig. 1-A) and if the number of earthquakes likely to occur in any magnitude range is N, then the number of earthquakes likely to occur in this magnitude range in each small division or block of a source area is

$$\frac{N}{n} \tag{2}$$

If seismicity is distributed along a fault of length L, the distribution of earthquakes is somewhat more complicated. We have used the relationship between fault rupture length (L) and magnitude (M) suggested by Mark (1977):

$$\log (L) = 1.915 + 0.389\,M \tag{3}$$

where L is the average fault rupture length in meters and M is as already defined. If there are $N_{M_2-M_1}$ earthquakes in the magnitude interval M_2-M_1 that have an average length of rupture (determined from equation 3) of L_{ave} and we are modeling a fault of length X, the earthquakes are distributed at the rate of

$$\frac{N_{M_2-M_1}}{X-L_{ave}}$$ (4)

earthquakes per unit of length along the fault. If one end of a fault is located at X_1 and the other end at X_{2-}, the earthquake rupture centers are assumed to occur uniformly

between $X_1 + \dfrac{L_{ave}}{2}$ and $X_2 - \dfrac{L_{ave}}{2}$ along the fault.

GROUND-MOTION ATTENUATION MODEL

The ground-motion attenuation function is a critical component of the probabilistic ground-motion mapping procedure. (See fig. 1-C.). Research has shown that much of the variability in estimates of peak ground-motion values is due to uncertainties inherent in ground-motion attenuation models (Bender, 1984; McGuire and Shedlock, 1981). While there are a number of published attenuation models available for various tectonic settings and applications (see for example, Campbell, 1984a), choice of a single, correct model for western Saudi Arabia is hindered by lack of strong-motion recordings and lack of reliable isoseismal maps due to a relatively low rate of earthquake activity and a sparse population distribution. Hence, there is no direct sampling of the propagation path of earthquake waves within this region. This lack of data leaves a fundamental question as to whether the region is characterized by high, low, or moderate attenuation. Our approach is to investigate the ground-motion hazard implications of both a conservative low- attenuation model (high Q) and a preferred high-attenuation model (low Q), thereby, providing upper bound and preferred ground-motion estimates within the constraints of seismic source zones and seismic activity rates of this study.

PROBABILITY DISTRIBUTION OF GROUND MOTION

Once the seismic activity rate per unit area or per unit length of fault is determined for the seismic source zones of the region, and a ground-motion attenuation function is decided upon, a distribution of ground motion is calculated (fig. 1-D) for a number of individual sites located on an appropriate grid pattern (fig. 1-A) throughout the region.

From the distribution of ground motion at each site (fig. 1-D), it is possible to determine directly the expect.de number of times a particular amplitude of ground motion is likely to occur in a given period of years at a given site, and, thereby, the maximum amplitude of ground motion in a given number of years corresponding to any level of probability (fig. 1-E). The relationship between return period $R_y(a)$, exposure time, T, and probability of exceedance during that exposure time, $1-F_{max,t}(a)$ is explained by the following development.

First, the distribution of the expected number of occurrences of ground motion at each location is calculated. The peak ground motion, for example, the peak acceleration corresponding to some extreme probability, is then calculated from the distribution of the expected number of occurrences in the following manner. Let the peak acceleration be a, then

$$F(a)=P[A<a \mid M>M_{min}]$$ (5)

is the probability that an observed acceleration A is less than or equal to the value a, given that an earthquake with magnitude M, greater than some minimum magnitude of interest, has occurred The calculation at a given grid point or along a fault is performed for every acceleration a of interest using:

$$F(a) = \frac{\text{expected number of occurrences with } A<a \text{ and } M>M_{min}}{\text{total expected number of occurrences } (M>M_{min})}$$

A typical F(a) is shown in figure 1-D.

F(a) is the probability that the acceleration value a will not be exceeded, given that an earthquake larger than the minimum magnitude occurs in the source zone. Therefore (1.0 - F(a)) is the probability that a WILL BE EXCEEDED. If ϕ is the yearly rate at which earthquakes larger than the minimum magnitude occur in the zone, then the expression

$$\phi \cdot (1.0 - F(a)) \tag{6}$$

gives the ANNUAL RATE at which earthquake accelerations greater than a occur. In T years,

$$T \cdot \phi \cdot (1.0 - F(a)) \tag{7}$$

gives the EXPECTED NUMBER OF OCCURRENCES of accelerations greater than a for a period of T years. If earthquake occurrences are rare, and the annual rate of occurrence is the same from year to year (that is, for Poisson occurrences), then probability theory tells us that

$$\exp(-(\text{expected number})) \tag{8}$$

is the probability that no such occurrence happens. Thus, the probability that acceleration value a is not exceeded in T years due to an earthquake in the source zone considered is given by the expression

$$\exp(-T \cdot \phi \cdot (1.0 - F(a)))$$

which can be rewritten as,

$$F_{max,t}(a) = e^{-\phi t[1-F(a)]} \tag{9}$$

where T now equals a particular exposure time, t. Using (9), a table of (a) and F(a) is constructed. For a particular exposure time T=t, $F_{max,t}(a)$ is calculated, and the value of a for a given extreme probability, say $F_{max,t}(a)$=.90, is found by interpolation.

It is convenient here to define the term return period as:

$$R(a) = \frac{1}{1-F(a)} \tag{10}$$

6

where $R(a)$ is the average number of events that must occur to get an acceleration exceeding a. The return period in years is given approximately by

$$R_y(a)= \frac{R(a)}{\text{Expected number of events per year } (M \geq M_{min})} \qquad (11)$$

We obtain from (10) and (11):

$$\phi t(1-F(a)) = \frac{t}{R_y(a)} \qquad (12)$$

thus, from (9) and (12): $F_{max,t}(a)=e^{-t/R_y(a)} \qquad (13)$

and $\ln(F_{max,t}(a))=- \frac{t}{R_y(a)} \qquad (14)$

For an extreme probability of 0.90 and an exposure time of t=100 years:

$$\ln(.90)=- \frac{100}{R_y(a)}$$

or

$$R_y(a)= \frac{100}{.1054} =949 \text{ years}$$

Thus, the average return period for the ground motions we have mapped is about 950 years.

It may be useful to point out that using equation (13) and setting the exposure time equal to the average return period $R_y(a)$; that is

$$t=R_y(a),$$

we have $F_{max,t}(a)=e^{-1}=0.37. \qquad (15)$

Thus the acceleration with a return period of $R_y(a)=t$ years has a probability of

$$1-F_{max,t}(a)=1-0.37=0.63 \text{ or } 63 \text{ percent}$$

of being exceeded in t years. The point is that accelerations (or any other parameter) with a particular return period have a 63-percent probability of being exceeded during an exposure time equal to that return period.

Frequently, it is convenient to express the maximum ground motion in terms of the annual probability of exceedance. Let $r_T(a)$ be the probability of exceedance of ground motion a in T years; then

$$F_{max,\ T}(a)=1-r_T(a)=e^{-T/R_y(a)} \qquad (16)$$

and
$$r_T(a)=1-e^{-T/Ry(a)} \qquad (17)$$

for T = one year, (17) becomes

$$r_T(a)=1-e^{-\frac{1}{Ry(a)}}$$

when $R_y(a)$ is sufficiently large (say, greater than 10 years),

$$r_T(a)=\frac{1}{R_y(a)}$$

TECTONIC SETTINGS OF THE SEISMIC SOURCE ZONES

DEAD SEA RIFT

The Dead Sea rift is a 1,000-km long, sinistral-slip boundary between the Arabian and Sinai plates (fig. 2). Although commonly referred to as a rift, the structures defining the plate boundary result from transform movement along a shear zone connecting the Red Sea spreading ridge with the Zagros collisional zone of Turkey. Inception of shear movement coincides with initial rifting of the Red Sea in pre-Miocene time and offset Precambrian through Cretaceous rock units indicates about 105 km of cumulative left-slip movement. The average slip rate is estimated to be 0.7-1.0 cm/yr over the last 4-5 m.y. Late Quaternary fault displacements have been mapped along the length of the transform boundary (Garfunkel, 1981); however, structural style and trend, and contemporary seismic activity vary considerably. We have, therefore, segmented the transform plate boundary into three separate source zones to reflect these differences (fig. 3). A growing body of knowledge indicates that discrete segments of large strike-slip faults possess varying seismological characteristics generally governed by large scale crustal asparities and varying strike of the fault trace within a uniform, regional stress regime (Sykes and Seeber, 1982; Sieh, 1981; Nishenko and McCann, 1981; Sykes and Nishenko, 1984). A description of the three source zone segments, from south to north, follows: (a) the Gulf of Aqaba-Arva Valley, (b) the Dead Sea rift, and (c) the Lebanon Mountains segments. Finer distinctions than used in this study could perhaps be made in the Dead Sea rift and the Jordan fault segments because of subaerial exposure of most of the fault system and a larger number of earthquakes recorded in this region. However, because this study concerns western Saudi Arabia, finer distinctions in seismic sources in the central and northern fault segments would have little influence on ground motions affecting northwestern Saudi Arabia.

Gulf of Aqaba (Elat)

The Gulf of Aqaba (fig. 2) is the widest and deepest segment of the transform plate boundary and is characterized by the structural development of en-echelon rhomb-grabens (pull-apart basins). Three such grabens have been inferred to underlie the Gulf of Aqaba, each filled by a few kilometers of sediment (Garfunkel, 1981). Rhomb-graben development is a common structural style along transform plate boundaries where the strike of the transform deviates from the regional slip direction and have been long recognized in the United States as important structural elements along the transform plate boundary of southern
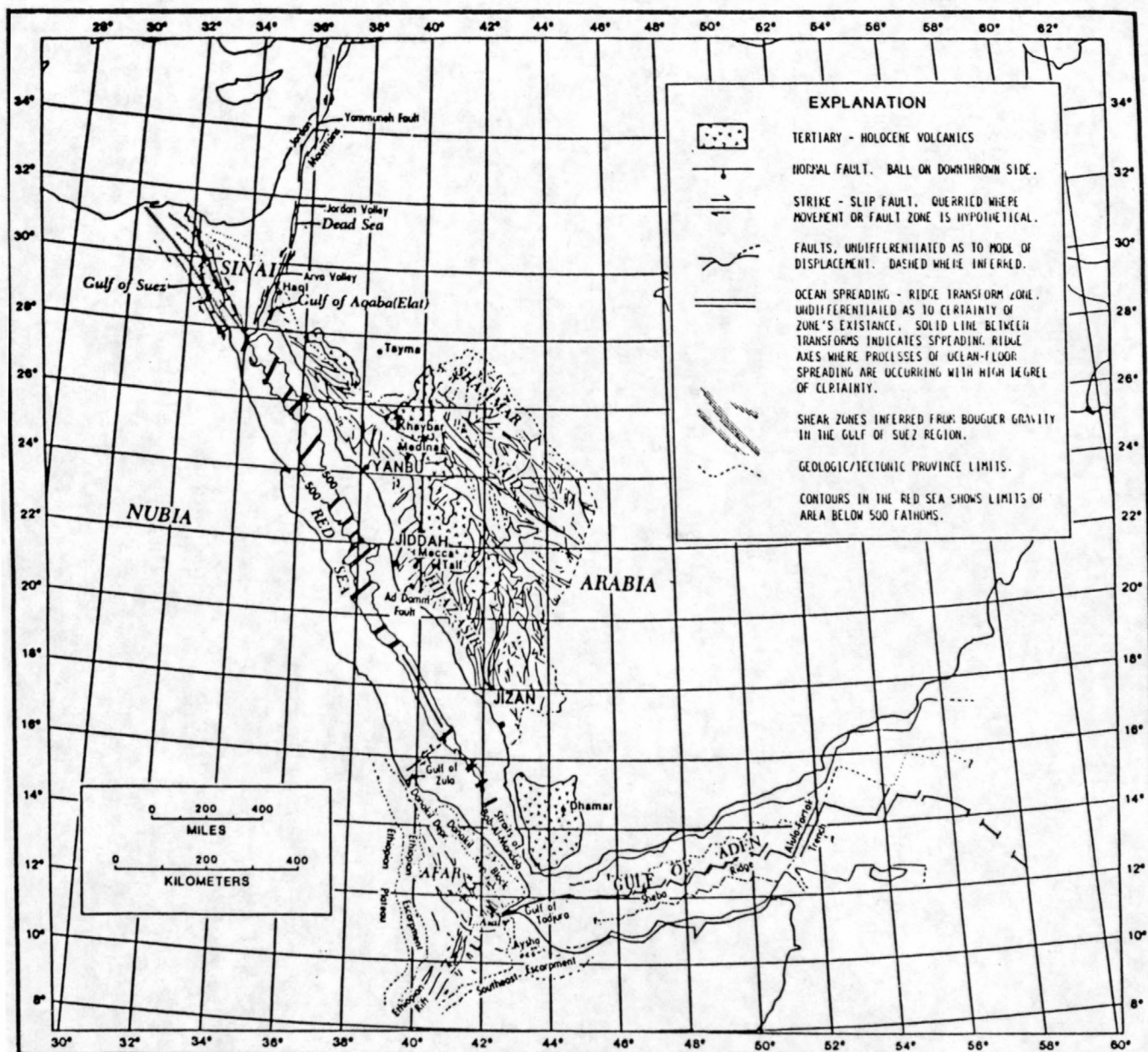
Figure 2.--*Index map of selected tectonic, geologic, and geographical features and sites referenced in the text. Sources of map compilation by region: (1) Western Arabia peninsula: Ministry of Defence, United Kingdom (1980), Brown (1972), Greenwood and others (1980), Coleman (1973), Merghelani and others (1981); (2) Dead Sea Rift: Garfunkel (1981), Eyal and others (1981), Garfunkel and others (1981); (3) Gulf of Suez: Garfunkel and Barton (1977), Riad (1977); (4) Red Sea: Drake and Girdler (1964), Hall (1980), Coleman (1973); (5) Gulf of Aden: Laughton (1966), Laughton and others (1970), Cochran (1981, 1982); (6) Afar: Kronberg and others (1975), Barberi and others (1975).*

9
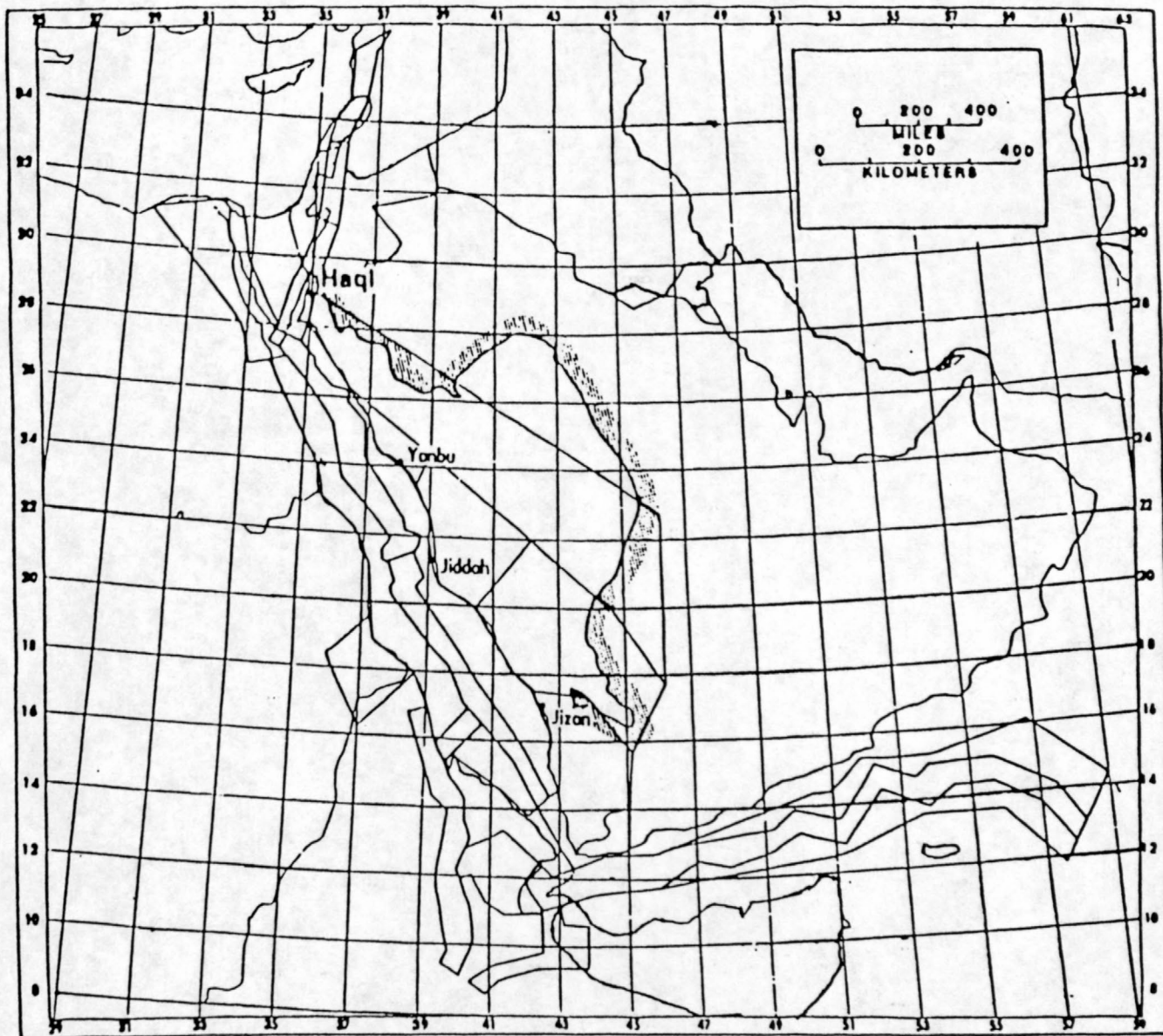
Figure 3.--*Seismic source zones of the Arabian shield, Red Sea rift, and contiguous tectonic systems used in this study.*

California (Crowell, 1974). Local extension across the transform zone results in small magnitude crustal separation and a "leaky" transform boundary. Garfunkel (1981) estimates 35-40 km of young slip is adequate to open the rhomb-grabens of the Gulf of Aqaba. Crustal separation across the transform boundary is estimated to be about 1 km in the central and southern segments. Older, Miocene and post-Miocene slip was distributed throughout a broader region of shear neighboring the gulf. Sinistrally offset Miocene dikes intruded in the Precambrian crystalline rocks of eastern Sinai suggest 24-km cumulative post-Miocene offset on a shear system of a anastomosing strike-slip faults in a 30-km-wide zone neighboring the gulf (Eyal and others, 1981). Similar displacement Is estimated for the eastern coast of the Gulf of Aqaba (Eyal and others, 1981). Thus, some 60 km of the total 110-km offset along the transform system is taken up by faults within the gulf itself. North of the Gulf of Aqaba, faults of the Dead Sea transform boundary are subaerially exposed In the Arva Valley. Active en-echelon left-slip faults are evident within this topographic saddle while normal-slip faults delimit some of the margins (Garfunkel, 1981). In the northern Arva Valley, the Arva Valley fault bounds the eastern margin of the topographic depression and has a distinct topographic expression and late Quaternary movement over a length exceeding 100 km (Garfunkel and others, 1981; Garfunkel, 1981).

Dead Sea Basin

The trend of the transform boundary shifts from a predominant north-northeast trend through the Gulf of Aqaba-Arva Valley structural trends to a predominant north-south trend along the Dead Sea basin (fig. 2). Topographically, the Dead Sea occupies the lowest portion of the subaerially exposed transform boundary. The Arva fault bounds the east side of the Dead Sea basin, but structural expression of the fault diminishes to the north. The Jordan (Jericho) fault, a major sinistral fault en-echelon to the Arva, bounds the Dead Sea basin to the west. The Dead Sea occupies a rhomb-graben between the two sinistral slip faults. Trenching studies across the Jordan (Jericho) fault indicate two large earthquakes in the past 2,000 yrs; one event occurring between 200 B.C. and A.D. 200 and one between A.D. 700 and A.D. 900 (Reches and Hoexter, 1981). Other, smaller events could be inferred. Precise dating of the events is precluded because of poor soil development and the predominance of coarse clastic deposits in the region. Left-lateral distortion and dislocation of walls of an 8th century palace located somewhat west of the main trace of the Jordan fault (Reches and Hoexter, 1981) indicate that not all of the shear strain is accommodated along the main trace of the Jordan fault, but distributed throughout a broader area of the Jordan Valley. Average slip rate on the Dead Sea portion of the transform is estimated to be 0.7 cm/yr (Reches and Hoexter, 1981), consistent with the average slip of the overall plate boundary of 0.7-1.0 cm/yr. The Jordan fault continues northward through the Jordan Valley to the Sea of Galilee. Mountain fronts on either side of the Jordan Valley are fault controlled and, locally at their base, scarps attain several tens of meters in height (Garfunkel and others, 1981). Within the valley near the Jordan fault trace, lacustrine beds are tilted at 30° and, locally, are gently folded up to a few hundred meters from the fault indicating a small amount of compression across the fault (Garfunkel and others, 1981).

11

North of the Jordan Valley, the transform boundary splays into three large fault strands. (See fig. 2.). The central strand, the Yammuneh fault, follows a sinuous course northward through the Jordan Mountains. The sharp easterly bend in the transform boundary through this segment results in a strong constraining bend in the left-slip transform system. The resulting transpression is postulated as causing large topographic uplifts on either side of the fault (Quennell, 1959). The other two large splay faults may also be active, but their surface trace dies out some 50-60 km north of the Jordan Valley (Garfunkel and others, 1981).

Ben-Menahen (1981) noted a nonuniform distribution of seismic slip along the length of the Dead Sea transform. While moderate-to-large earthquakes have occurred in all of the above three segments of transform zone, historic and contemporary microseismic activity are considerably lower in the Gulf of Aqaba-Arva Valley segment as compared to the central and northern segments. Lack of historically reported large earthquakes (M>7) in the southern segment could be due to the historically sparse population of this region; however, low levels of microseismic activity recorded during recent monitoring tends to support the general distribution of the macroseismic data (Ben-Menahem and Aboodi, 1981). Ben-Menahem (1981) concluded that a large portion of the total slip is accommodated aseismically in the south, whereas to the north, as the Zagros collisional zone is approached, slip becomes purely seismic. This thesis is consistent with the tectonic style of the transform boundary in its northern segments. North of the Dead Sea, compression across the transform boundary increases considerably because of the large constraining bend through the Jordan Mountains resulting, perhaps, in predominantly stick-slip fault movement. The tectonic setting is generally similar to the "big bend" region of the San Andreas fault in southern California that broke in 1857 in a great earthquake and has a prehistoric history of characteristically breaking in large events (Sieh, 1978). Sykes and Seeber (1982) refer to these large bends in transform boundaries as tectonic knots and conclude that they are areas of considerable stress accumulation because of their difficulty in accommodating relative plate motion.

Fault-Source Model for the Dead Sea Rift

The three segments of the Dead Sea rift are modeled as mixed-source types of seismic source zones (fig. 1-A); that is, linear fault-rupture sources are modeled within a broader area source (fig. 4). Earthquakes $M_s>6.5$ are modeled as two-dimensional sources whereas earthquakes $M_s<6.5$ are modeled as point sources throughout the area source. Two fault sources are modeled 20 km apart and central to the area source. Double, parallel faults were modeled in each of the three segments to better represent the en-echelon nature of long Quaternary strike-slip faults (that generally bound rhomb-grabens) and to account for deformation extending beyond a single fault trace.

GULF OF SUEZ

As in the case of the Dead Sea transform (fig. 2), additional detail in seismic source zones could perhaps be provided for eastern Egypt. However, because additional detail in source zones of this region would have little affect on resulting ground motions in extreme northeastern Saudi Arbia, we have not attempted detailed zones in this region.
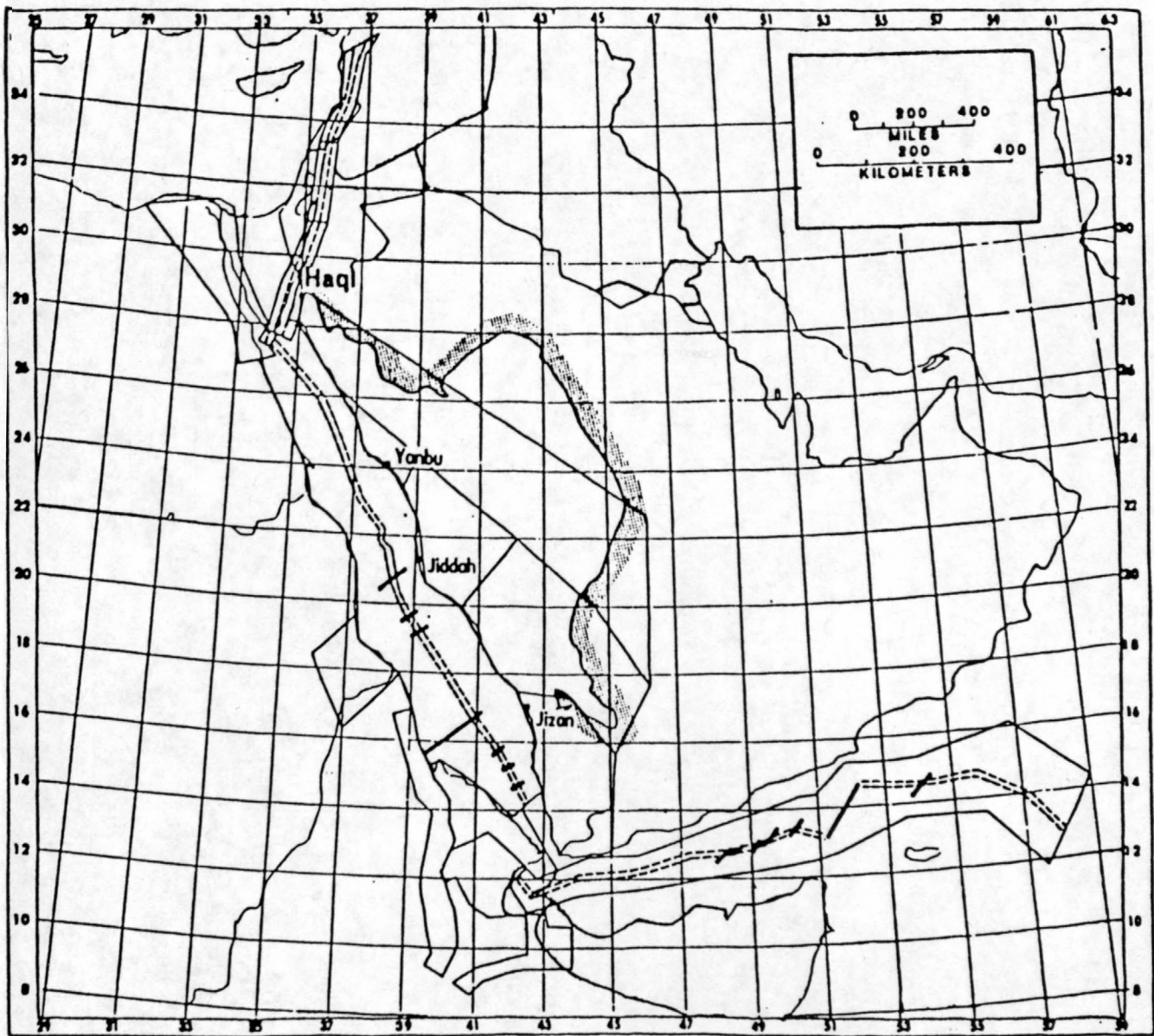
Figure 4.--*Fault-source model for the Dead Sea-Red Sea-Gulf of Aden rift system used in this study.*

13

Age of incipient rifting along the Suez arm of the Red Sea rift is not precisely known, however, stratigraphic evidence indicates rifting was well underway by late Oligocene to early Miocene (30-20 m.y. B.C.) (Garfunkel and Bartov, 1977). An estimated 15-20 km of crustal stretching in the southern part of the rift was accommodated through faulting and block tilting. However, crustal separation was too small to result in production of oceanic lithosphere between the Sinai and Nubian plates (Garfunkel and Bartov, 1977). Amounts of crustal stretching decrease northward along the rift.

While the primary episode of deformation along the rift was completed by late Miocene time, slow subsidence of the gulf has continued through the Quaternary. Quaternary fault scarps are generally concentrated along a central trough and along the eastern border fault (Garfunkel and Bartov, 1977), and they retain a zig-zag pattern inherited from middle Tertiary structural fabric. Young uplift of the rift margins is indicated by fragmentary evidence of uplifted marine terraces and reefs (Garfunkel and Bartov, 1977) neighboring the southern part of the rift.

North of the gulf, structures of the rift are covered by aeolian dunes and deltaic deposits of the Nile River. However, a continuous physiographic depression persists northward along a projection of the central trough; it forms the physiographic furrow in which the Suez Canal was excavated. Some of the topographically low areas of this depression are below sea-level, and Garfunkel and Bartov (1977) argue that stratigraphic evidence, together with the geomorphic evidence, indicates young subsidence of the canal depression where continental and pluvial sedimentation has generally kept pace with subsidence.

The structural framework of Egypt is complex with four primary, intersecting fault trends being recognized throughout this region. These are the east African fault systems trending north-south, the Erythrean or African fault system trending northwesterly, east-west Tethyan faulting, and the Aualitic faults trending northeast southwest (Said, 1962; Riad, 1977). Riad interpreted a number of northwest-trending, parallel to subparallel shears in northern Egypt based on a Bouger gravity anomaly map of the region (fig. 2). He inferred right-lateral movement across the shear zones based on space-photography and suggestions of independent stratigraphic studies. The northwest strike of the shear zones and dextral sense of movement would be conjugate to the sinistral, northeast-trending Dead Sea transform. Opening of the Gulf of Suez is suggested to have resulted from dextral slip along the shear zones.

The Gulf of Suez seismic source zone is drawn to include those shear zones inferred to be associated with the gulf (fig. 3). The eastern boundary of the zone has been extended northward to include the topographic depression of the Suez Canal. The zone collects a number of historically reported earthquakes in northern Egypt assessed as high as Modified Mercalli intensity X (Poirier and Taher, 1980). It is assumed that seismic potential is uniform throughout the zone although this, in fact, is not entirely clear. Structural deformation is most intense in the Gulf of Suez in the southern part of the source zone; however, historically reported events concentrate in the northern half of the zone. This may be a result of longer settlement of the Nile delta region as compared to the desert regions neighboring the Gulf of Suez.

14

Drake and Girdler (1964) recognized three physiographic provinces of the Red Sea (fig. 2). These are the coastal shelves, a broad main trough, and a deep axial trough. The three provinces are present to varying degrees along the length of the Red Sea. North of lat 24° N., an axial trough is not clearly developed and the shelf areas are quite narrow. Between lat 19° N. and 24° N., an axial trough is characterized by a discontinuous series of "deeps" in excess of 1,000 fathoms, and a main trough is well developed. South of lat 19° N., shelf areas are broad and the axial trough has a continuous, narrow expression to about lat 15° N. where the main trough shoals into the Straits of Bab-al-Mandab.

Structural deformation is intense in the axial zone and characterized by numerous normal faults (Ross and Schlee, 1973, 1977; Phillips and Ross, 1970). Marginal to the axial trough, deformation of the main trough is less intense but still characterized by abundant normal faults and folds. Many shallow folds are related to salt flowage and diapirism (Ross and Schlee, 1973, 1977). The transition from axial trough to main trough (roughly following the 500-fathom bathymetric contour) is marked in places by narrow, intensely faulted zones or large downfaulted blocks (Ross and Schlee, 1973, 1977). Shelf areas are generally characterized by normal faults (more prevalent in the southern Red Sea) and folds related to salt flowage and diapiric intrusion.

The Red Sea was recognized early in the development of global plate tectonic theory as an extension of the worldwide rift system (Sykes, 1967); however, important aspects concerning the rifts' fundamental crustal structure and tectonic development remain uncertain and are topics of much debate in recent geological literature. Central to the debate is the nature of the crust beneath the broad shelf areas of the southern Red Sea. One school of thought holds that the shelf areas in the southern Red Sea are underlain by Miocene age oceanic crust or, at least, mantle derived crust while a second school of thought argues that the shelf areas are characterized by rifted and extended continental crust. While it is generally accepted that ocean-floor spreading (creation of new oceanic crust) has been occurring in the axial trough of the southern Red Sea (south of about lat 19.5° N.) since Pliocene time, a variety of geological, geophysical, and plate kinematic arguments have been proposed both suggesting and denying the possibility of early Miocene ocean-floor spreading.

Magnetic signatures obtained across the shelves are subdued due to an approximate 3-km thick Miocene evaporite sequence that also precludes direct observation of deeper basement structure through standard seismic-reflection techniques. Broad, linear magnetic anomalies on the shelves have an abrupt transition to high-frequency anomalies in the coastal plain of southwestern Saudi Arabia. The abrupt transition in signature has commonly been interpreted as the contact between oceanic and continental crust (Gettings, 1977; Hall, 1980; Hall and others 1977; Girdler and Styles, 1974). Furthermore, these investigators suggest that the low-amplitude broad wavelength anomalies of the shelves are roughly symmetric about the axial trough and generally correlate with Miocene age anomalies of the Heirtzler and others, (1968) magnetic time scale. Alternatively, Cochran (1983), following Fraziers' (1970) structural interpretation of an area off of northern Afar, suggests that the offshore total intensity magnetic anomalies are due to salt diapirs along large basement faults and, hence, cannot be correlated with ocean-floor-spreading anomalies. Cochran (1983) further notes a correlation of total intensity magnetic anomalies with free-air gravity anomalies which he states would not be expected if the magnetic

anomalies were spreading anomalies, but would allow the interpretation that the magnetic signatures derive from faulted basement and salt structures.

Recent plate kinematic reconstructions (Le Picheon and Francheteau, 1978; Cochran 1981, 1983), while applying different fundamental contraints on the amount of rotation of the Arabian and Nubian plates about the Euler pole of McKenzie and others (1970), and using different interpretations of the total number of rigid plates in the region, require an amount of total plate separation in the southern Red Sea more than twice the width of Pliocene-precent ocean floor in the axial trough. The required extra space could be accommodated through pre-Pliocene ocean-floor spreading, extended and thinned continental crust, or any combination of unknown percentages of thinned continental crust and mafic intrusion. Abundant geologic evidence exists of significant amounts of mafic intrusion into the continental crust bordering the Red Sea (Schmidt and others, 1983; Blank, 1977). An unresolved issue, however, is the lateral extent of extended continental crust. In models that incorporate Miocene age ocean-floor spreading, this zone is relatively narrow and outcrops immediately east of the coastal plain (Schmidt and others, 1983). Alternatively, in Cochran's (1983) interpretation, extended continental crust extends far seaward, beneath the shelves and main trough of the southern Red Sea. Furthermore, the floors of the central and northern Red Sea are suggested to be extended continental crust as Cochran (1983) argues that organized ocean-floor spreading has not yet commenced north of about latitude 21^0 N., although the region between 21^0 N. and 25^0 N. is suggested to currently be in transition from diffuse continental extension to an ocean-floor spreading mode of plate separation.

Bohannon (1985) has suggested a tectonic model of early Red Sea rift development that incorporates lower to middle crustal expansion through large-scale mafic intrusion with concomitant brittle extension in the upper crust. The magnitude of brittle extension is suggested to be about 40 percent; a relatively small value in comparison to estimates of over 100 percent extension along some passive continental margins (LePichon and Sibuet, 1981). Incorporating geologic interpretations from field mapping with an interpretation of a seismic-refraction profile (Mooney and others, 1985) that extends across the southern Arabian shield to the Farasan Islands, Bohannon (1985) envisions brittle extension accommodated by widely spaced up-to-basin listric normal faults above an east-dipping low-angle detachment that outcrops near the eastern coastal plain and roots beneath the Arabian Escarpment. The brittlely extended crust is exposed in a 75-km-wide belt east of the coastal plain and exhibits characteristic arcuate traces of normal faults. While Bohannon (1985) suggests it is possible that extended continental crust exists beneath the coastal plain, he argues that west of the coastline the crust is of oceanic character.

The regional distribution of seismicity throughout the Red Sea has changed little since the early investigations of Gutenberg and Richter (1954), Drake and Girdler (1964), and Sykes and Landisman (1964). Notably, with an additional 20 yrs of data and establishment of the Worldwide Standard Seismograph Network (WWSSN) seismicity remains concentrated proximal to the southern Red Sea rift (Fig. 5). Relocation efforts have refined post-1955 earthquake locations to an accuracy of 10-20 km (Sykes and Landisman, 1964; Fairhead and Girdler, 1970) for moderate and large shocks in the region. Reasonable associations with at least region-scale structure can, therefore, be inferred. A large aftershock (M_b=5.3) of the North Yemen earthquake of December 13, 1982, was recorded by the WWSSN and a network of portable seismographs deployed in the epicentral region (Langer and Merghelani, 1983). The epicenters determined independently by local and

16

teleseismic data are no more than 5 km apart, suggesting that contemporary seismic activity in this area can be reliably determined from WWSSN data.

While seismic activity is concentrated in the southern half of the Red Sea and predominantly confined to the axial trough, the seismicity is not uniformly distributed throughout this area. Some earthquake activity is clustered on, or near, inferred transform faults of the rift axis (fig. 5). Focal mechanisms for two earthquakes located near the southern Red Sea rift axis indicate nearly pure strike-slip movement on northeast-trending planes and suggest contemporary seismic activity on rift transform faults (Fairhead and Girdler, 1970). Other significant activity appears to occur along other portions of the central rift not having recognized transform faults. This activity may be related to either intrusive activity along the axial trough, normal fault movement associated with the downdropping of blocks into the axial trough, or movement along presently undetected transforms.

Figure 3 shows the seismic source zone configurations of the Red Sea used to group historic seismicity for the determination of earthquake recurrence rates. Three primary zones have been constructed. A relatively narrow zone based on the 500-fathom bathymetric contour includes seismicity associated with the highly faulted axial trough. This central-rift zone has been subdivided into northern and southern halves based on a significant decrease in observed seismicity north of latitude 21° N. Distinguishing these two segments preserves the influence of the seismically active southern axial trough in the seismic-hazard maps. In the northern half, while an axial trough is not well-defined north of lat 24° N., the few epicenters that are present are contained by the 500-fathom contour. The broad zone, spanning the width of the Red Sea, is intended to separate primary, rift-related crust and structure of the main trough and shelves from predominantly Precambrian crust and structure of the Arabian and Nubian shield areas. Because of the previously discussed conflicting interpretations of offshore crustal structure, the eastern boundary of this zone can be interpreted in several different ways. Considering hypotheses advocating a primary plate separation mode of ocean-floor spreading, the zone boundary approximates the full extent of inferred Miocene age oceanic crust. Under the hypothesis of deep-to-middle crustal expansion through massive diking, the zone boundary separates crust of mantle derivation to the west from continental crustal structure to the east. Considering hypotheses of rifted continental crust extending beneath the shelf areas to the margins of the axial trough, the zone boundary separates the region of significant brittle crustal extension from less deformed regions on shore. Under this last hypothesis the definition of the zone boundary is a matter of degree of deformation, and the boundary becomes arbitrarily located.

Fault-Source Model for the Red Sea Rift

The fault-source earthquake model for the Red Sea rift (fig. 4) is developed from fundamental plate tectonic concepts that serve to explain tectonic processes of active oceanic spreading ridges. The block diagrams of figure 6 schematically illustrate these concepts. First, although the locations of evolving spreading ridges and transforms may be predisposed by ancient structures of the Precambrian continental crust (Sykes, 1978), once ocean-floor spreading is established, structures of the continental and oceanic domains are geologically distinct. Second, once organized ocean-floor spreading is established, seismically active transform faults exist between offset spreading ridges and have earthquakes that exhibit strike-slip focal mechanisms. Wilson (1965) first introduced this concept. Recent microearthquake studies using ocean-bottom

17
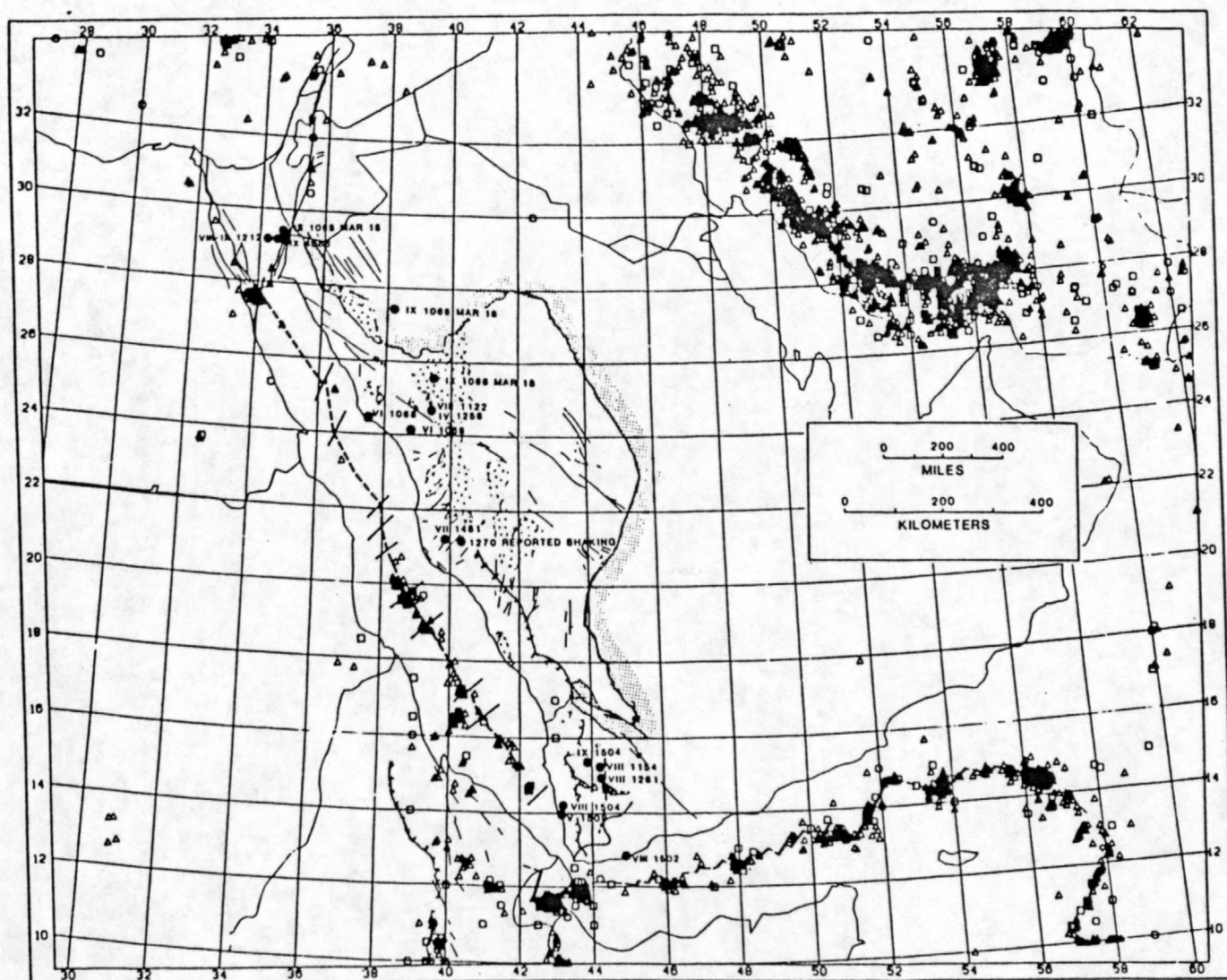
Figure 5.--*Preliminary map of seismicity of Saudi Arabia and adjacent regions. Computer-generated symbols arc earthquakes obtained from the NEIS worldwide seismicity catalog. Modified Mercalli intensities are from Poirier and Taher (1980) and are plotted only for the western Arabian peninsula. Locations of intensity values do not necessarily represent epicenter locations. They represent locations of existing reports of shaking effects which may be distant from actual epicenters due to very low population density in western Saudi Arabia. Earthquake symbols represent the following values: Triangles = $4 \leq M < 5$; squares = $5 \leq M < 6$ hexagons = $6 \leq M < 7$; diamonds = $7 \leq M < 8$; hourglass = $M \geq 8$.*

seismographs (OBS) have shown this distribution of seismicity to be generally characteristic of oceanic transforms (Francis and others, 1978; Forsyth and Rowlett, 1979; Project Rose Scientists, 1981; Rowlett, 1981). Other information gained from OBS monitoring indicates that seismicity is distributed across the interior plate corners of some ridge-transform intersections. At the regional scale of this investigation, however, this detail is not significant to the fault source model. A third point, not well illustrated by figure 6, is the characterization of ridge-crest earthquakes by normal focal mechanisms oriented parallel to the ridge strike (Sykes, 1967; Trehu and others, 1981). A useful generalization is that the larger spreading-ridge earthquakes, at any given spreading rate, occur off the spreading-ridge axis by perhaps 10 km or more (Solomon and Burr, 1979; Burr and Solomon, 1978). While observed spreading-ridge earthquakes can neither confirm nor deny this generalization, Solomon and Burr (1979) suggest this to be a reasonable assumption based on considerations of observed high heat flow and very thin crust directly within axial troughs.

These concepts and generalizations have been derived from studies of mature ocean-spreading systems worldwide, and it is not entirely clear that they can be applied in a strict sense to the incipient ocean-spreading system of the Red Sea. Conflicting interpretations of the composition and structure of the crust neighboring the axial trough of the southern Red Sea and the unresolved mode of plate separation in the northern Red Sea (brittle extension vs. ocean-floor spreading) raise uncertainties in developing a fault-source earthquake model based on worldwide examples of mature ocean-spreading ridges. Because of the youth of the Red Sea rift, an axial rift valley is incompletely developed, and offsets of the axial trough centerline (assumed centerline of rift spreading) across inferred transforms are extremely small, being less than 15 km (Coleman, 1977) as compared to hundreds of kilometers for some mature spreading systems (Stewart, 1983). The specific geometry of the Red Sea ridge-transform fault system cannot be defined with confidence. Our approach, therefore, has been to style fault sources in accord with an ocean-spreading-ridge model but to relax some constraints of the rigid-plate transform theory illustrated in figure 6.

Earthquakes are modeled as linear fault ruptures on parallel, spreading- ridge faults modeled 10 km either side of the axial trough centerline as represented by Coleman (1977; fig. 4). Furthermore, in the southern Red Sea axial trough zone, transform faults as inferred by Hall (1980) have been modeled perpendicular to the spreading-ridge axis and include those identified with reasonable certainty as well as those that are speculative. These transforms have been modeled beyond the terminal ends of the offset axial trough centerline and extend across the entire width of the axial trough as defined by the 500-fathom bathymetric contour. No transform faults were modeled in the northern axial trough zone because the paucity of historically recorded seismicity in this region precludes the determination of seismic activity rates for such faults. A single exception is an inferred north- northeast-trending fault that follows a steep bathymetric break at the Gulf of Suez-Red Sea junction. An $m_b=6$ earthquake occurred at this location on March 31, 1969 (Fairhead and Girdler, 1970; Ben-Menahem and Aboodi, 1971), and the zone has remained intermittently active producing four earthquakes $m_b=4-4.5$ through 1984. The zones' unique structural setting and continuing history of seismic activity distinguishes it from other inferred structures of the northern Red Sea. We have, therefore, represented this seismically active zone as a distinct seismic source.

19
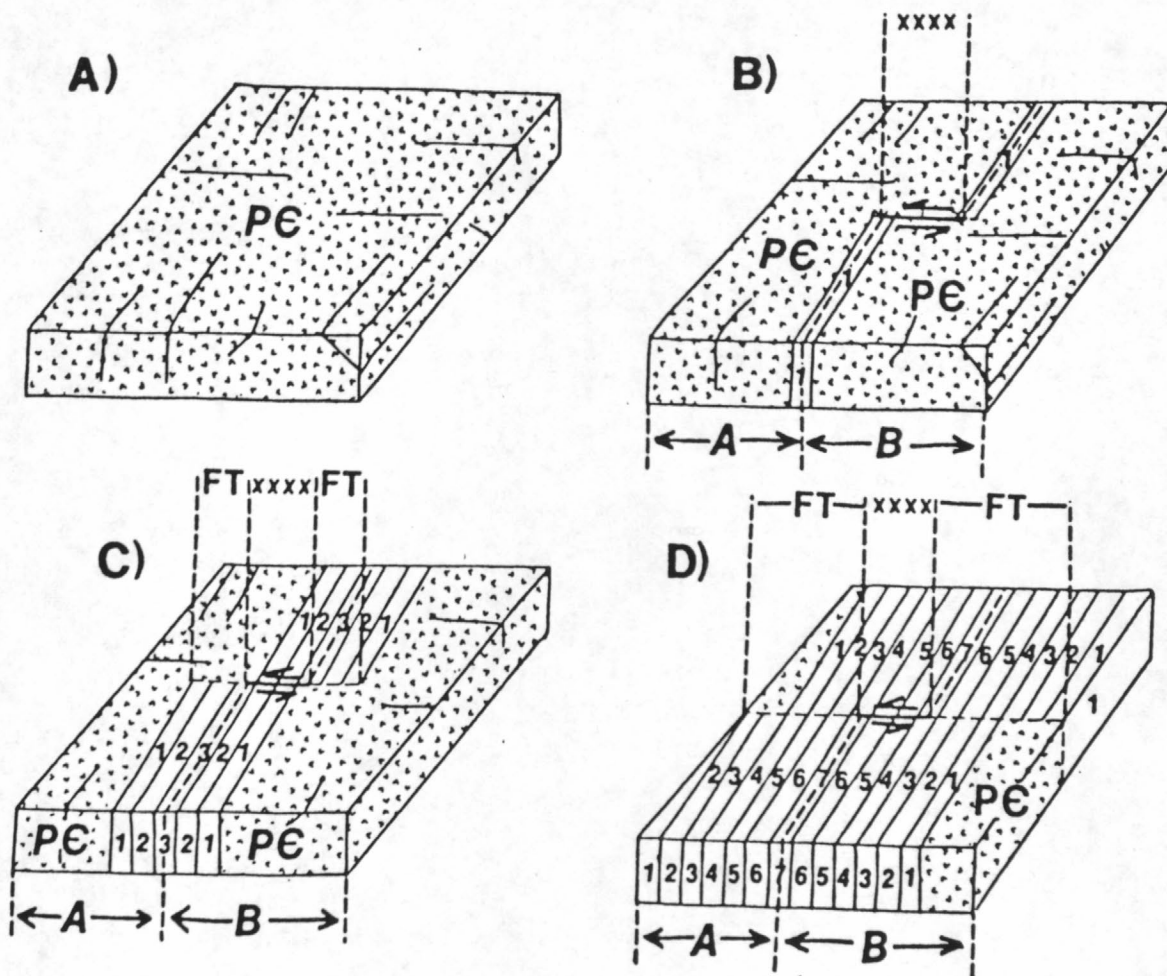
Figure 6.--*Schematic block diagrams showing formation of oceanic crust through rigid-plate rifting. A, Precambrian cystalline crust with preexisting structural fabrics and faults. Magnetic anomaly time, T=O. B, Magnetic anomaly time, T=1. Initial intrusion of oceanic crustal material along preexisting zones of weakness separates the Precambrian crust into blocks A and B. Dashed line indicates axial centerline of the new rift. Spreading is assumed to be symmetric to, and at a constant rate along, the rift axes. Creation of new crust across the right-hand offset of the spreading ridge is accommodated by left-lateral displacement along a transform fault. Zone of seismicity associated with transform movement extends between the spreading ridge axes and is shown by the line of "X's" raised out of the plane of the diagram. C, Magnetic anomaly time, T=3. Continued symmetrical spreading along the rift axis, in time, results in accretion of young oceanic crust to blocks A and B and fossil transforms (ft on diagram) beyond the offset of the ridge axes. Note that the length of active transform faulting has not changed. Note also that fossil transforms have not formed through shear movement, but rather; through simple accretion juxtaposing crusts of different ages and composition. D, Magnetic anomaly time, T=7. Continued symmetrical rifting results in a broad area of oceanic crust. Note that the active zone of transform movement has not changed from diagram B. Further note the growth of fossil transforms from diagram C.*

The Red Sea rift and the continental rifts of east Africa are joined to the worldwide rift system through the Sheba Ridge spreading center that extends the length of the Gulf of Aden (fig. 2). To the east, at about longitude 58° E., Sheba Ridge is terminated by right-lateral transform slip along the Owens Fracture Zone. To the west, Sheba Ridge shoals into the Afar region of east Africa where its structural expression as a distinct ocean-spreading ridge is lost in a broad region of distributed extension (fig. 2). Geomorphic expression of Sheba Ridge narrows from a 300-km-wide mountain range near the Owens Fracture Zone to a narrow valley occupying the Gulf of Tadjura, although expression of the axial valley does not greatly change (Laughton, 1966; Laughton and others, 1970). Numerous northwest-southeast-trending transform faults offset Sheba Ridge along its length (fig. 2); the most spectacular being the Alula-Fartak trench (Laughton, 1966) at latitude 52° E. where Sheba Ridge is offset a distance of 160 km. The transform is marked by a linear northwest-trending trench 240 km long, 16 km across, and 2,800 fathom deep (Laughton, 1966). Earthquakes associated with the trench show strike-slip mechanisms characteristic of oceanic transforms (Sykes and Landisman, 1964). Transforms and fracture zones of Sheba Ridge are typically characterized by linear northeast-southwest-trending zones of mountainous topography up to 16 km wide in the eastern gulf, but considerably wider in the western gulf. Bouguer gravity anomalies, magnetic anomalies, and crustal velocities from seismic-refraction studies indicate Sheba Ridge is underlain by oceanic crust as much as 10 m.y. B.P. (Girdler, 1970; Laughton and others, 1970; Cochran, 1981). Beyond the 10 m.y. B.P. magnetic anomaly, Cochran (1982) suggests a zone of diffuse continental extension and mafic dike intrusion throughout an 80-km-wide zone to the Arabia coast. Structure within this zone is suggested to have resulted from an early (10-15 m.y. B.P.) crustal stretching and attenuation episode preceding ocean-floor spreading (Cochran, 1982).

Most of the seismicity of the Gulf of Aden shows a close spatial association with the axial valley of Sheba Ridge and associated transform faults (Fairhead and Girdler, 1970; McKenzie and others, 1970; Sykes, 1970; Sykes and Landisman, 1964; fig. 5). Some seismicity, however, occurs in the region of mountainous topography off the spreading axis and may be related to block adjustments in this region or a small amount of distributed ocean-floor spreading (Sykes and Landisman, 1964; Sykes, 1967). The largest earthquakes to occur in the gulf are associated with the Alula-Fartak transform zone. Magnitudes (m_b) for events occurring in 1959 and 1967 were 6.7 and 5.8 respectively Sykes and Landisman, 1964; Fairhead and Girdler, 1970).

Two seismic source zones have been constructed in the Gulf of Aden (fig. 3). A central rift zone collects seismicity occurring in close proximity to the axial valley. Near long 46° E., a second, broader zone envelopes the central rift zone and collects seismicity occurring within the broad area of mountainous terrain neighboring the central rift. The source zones terminate at the Owens Fracture Zone to the east. To the west, the central rift zone extends through the Gulf of Tadjurah into the Afar beyond Lake Asal to include the Ghoubbet-Asal rift and associated seismic activity (Abdallah and others, 1979). Westward, beyond Lake Asal, seismicity becomes diffuse and structural expression of a primary rift zone is obscured by significant distributed extension throughout the Afar.

As in the Red Sea fault-source model, spreading-ridge earthquakes have been modeled as linear ruptures on faults placed parallel to, and 10 km either side of, the spreading axis of the Gulf of Aden (fig. 4). West of long 48° E., transform offsets are many but of very short lengths; generally less than about 20 km (Cochran, 1981). Because such short rupture lengths would have no effect on ground motion values onshore, they have not been modeled in this study. Between longitudes 48° E. and 54° E. relatively long transform offsets of Sheba Ridge are present (Cochran, 1981) including the Alula-Fartak trench. These longer offsets have been included in the fault model as northwest-southeast- trending faults having linear (two-dimensional) earthquake rupture (fig. 4).

AFAR DEPRESSION

The Afar depression (fig. 2) of northeastern Ethiopia is the subaerially exposed structural junction of the Red Sea, Gulf of Aden and East Africa rift systems. Because this unique tectonic setting provides direct observation of tectonic processes of a spreading-ridge triple-junction, many diverse geologic investigations have addressed the structural and tectonic evolution of this region (see for example, Pilger and Rösler, 1975). To review the many significant contributions to the tectonics and structure of this region is beyond the scope of this investigation. Because our area of interest is the Arabian Peninsula, we are concerned here with only far-field effects of earthquakes originating within the Afar, and much detail that could perhaps be modeled in seismic sources specific to the Afar region would have no effect on earthquake ground motions at distances with which we are concerned. The seismic source zones are, therefore, derived from only regional aspects of the tectonic setting.

The central Afar is a highly extended region characterized by a thin crust of mafic composition, voluminous Quaternary tholeitic volcanism, and intense normal faulting along north-northwest and northwest trends (Barberi and Varet, 1977; Mohr, 1975; Morton and Black, 1975; fig. 2). The region is conterminous to the inland extension of Sheba Ridge to Lake Asal that has been proposed by Abdallah and others (1979) based on contemporary extensional tectonism observed in the Asal-Ghoubbet graben and an associated well-defined seismicity trend. Northwest of Lake Asal, in the central Afar, seismicity is diffuse and two focal mechanisms in the region indicate east-west-trending planes of strike-slip displacement (McKenzie and others, 1970). In microplate kinematic models proposed by Barberi and Varet (1977) and LePichon and Francheteau (1978), zones of northeast-trending shear accommodate transform motion between offset, northwest-trending zones of extension.

The metamorphic continental crust of the Danakil block (fig. 2) marks the northeastern boundary of the Afar. In many tectonic models of this region, the Danakil block is inferred to be a splinter of continental crust separated from continental crust of the Nubian and Arabian plates by oceanic crust of the Afar depression to the southwest and that of the Red Sea to the northeast (LePichon and Francheteau, 1978; Barberi and Varet, 1977; Hall, 1980). Offset of the primary locus of spreading from the southern Red Sea to the Afar is inferred to occur by means of a transform zone through the Dahlac Islands, north of the Danakil block, to the Gulf of Zula (fig. 2). In contrast to the aseismic appearance of the shelf areas of the southern Red Sea, a strong zone of seismicity

extends across the western shelf in the vicinity of the proposed transform (fig. 5). We have modeled this inferred transform zone as a fault- source for earthquakes in this region.

The western and southern boundaries of the Afar depression are marked by relatively narrow, bedrock escarpment terranes which are transitional zones between the structurally low, strongly faulted, and extended central Afar region and the structurally high, little, deformed regions of the Ethiopia and Somalian plateaus (fig. 2). Large-displacement normal faults and, in places, up-to-basin block rotations along (listric?) normal faults characterize the general structure of the escarpment terranes (Zanettin and Justin-Visentin, 1975; Juch, 1975; Gouin and Mohr, 1964). The escarpments converge to the southwest and follow the margins of the Ethiopian rift into the East African rift system.

A strong north-south seismicity trend has long been recognized along the length of the Ethiopian escarpment (Gouin and Mohr, 1964). Gouin (1970, 1979) found the Ethiopian escarpment to be the most seismically active zone in Ethiopia. Only a few epicenters occur in close proximity to the southeast escarpment, although the Aysha Horst, bounding the extreme southeast Afar, appears to be associated with significant activity (fig. 5).

Our seismic source zones for the Afar region are quite general because we are only concerned with low levels of earthquake ground motions at large distances from earthquakes in this tectonically active region. The Ethiopia and southeast escarpments (including the Aysha Horst) comprise seismic source zones bounding the Afar region (fig. 3). The source zones are terminated at a rather arbitrary location to the southwest where they converge and funnel into the Ethiopian rift. At some point towards the southwest, presently undefined, it would appear that contemporary tectonism within the escarpments is no longer influenced by the distributed, extensional processes of the Afar but more closely related to the tectonics of the Ethiopian rift.

The central Afar has been separated from areas to the north and south based on fault trends and intensity of tectonism and a dispersed pattern of seismicity.

Dominant northeast and north-northeast fault trends of the southwestern Afar associated with the intersection of the Ethiopian rift (fig. 2) have been excluded from the central Afar seismic source. No significant seismicity has been historically documented in this region. To the north, sparse seismicity of the Danakil block and Danakil depression have been excluded from the central Afar source zone.

WESTERN ARABIAN PENINSULA

Precambrian crystalline basement is widely exposed throughout western Saudi Arabia (fig. 2) although large areas are covered by voluminous Tertiary basalts. Three Precambrian tectonic provinces have been recognized in the structural framework of the shield (Greenwood and others, 1980). The Najd fault system is the most prominent structural feature of the Arabian shield and comprises the youngest of three Precambrian tectonic provinces (Greenwood and others, 1980). Shear zones of the Najd system separate the Hijaz-Asir province to the southwest from the Shammar province to the northeast (fig. 2). At least four major northwest-trending left-lateral wrench zones of the Najd cross the shield from the northeast coast of the Red Sea to the southeast shield area where the fault system is concealed beneath Mesozoic sedimentary rocks. Cumulative Precambrian

23

left-slip on the Najd system is estimated to be about 240 km (Brown, 1972). Greenwood and others (1980) suggests that the Najd tectonic province is also structurally depressed because of the lesser area of exposed high-grade metamorphic rocks and larger area of unmetamorphosed rocks as compared to the neighboring Shammar and Hijaz-Asir provinces.

The Hijaz-Asir Precambrian tectonic province lies between the Najd fault system and the coastal plain (fig. 2). In the southeastern part of this province, braided north-trending fault zones predominate with complex patterns of left- and right-lateral, normal and reverse faulting (Greenwood and others, 1980). In the central part of the province, faults have a distinctive northeast-southwest trend. The Ad Damm fault (fig. 2) is a prominent structure of this region extending some 130 km to the northeast from the coastal plain to beyond Taif. Pallister (in press) has inferred right-lateral Precambrian movement on this fault. Significantly, Merghelani and others (1981) have noted a high level of contemporary microseismicity in the vicinity of the fault.

The Shammar tectonic province is exposed over a relatively small area of the extreme northeastern shield area and is characterized by north- and northeast-trending lineaments and granitic intrusions (Greenwood and others, 1980).

Contemporary seismic activity in the shield area appears low as no significant earthquakes have been recorded in this area since the establishment of the World Wide Standard Seismograph Network in the mid-1960's. However, historical accounts researched by Poirier and Taher (1980) indicate that strong earthquake shaking has been experienced at Khaybar, Tayma, and Yanbu in the year 1068 and Medina in 1122 and 1256 (figs. 2, 5). Taif experienced earthquake shaking in the year 1270 and Mecca in 1481. Detailed accounts for these events are not given by Poirier and Taher (1980): however, they do note that ground cracking and fissuring accompanied widespread destruction in Arabia in the 1068 event. They assigned a Modified Mercalli intensity IX to these reports of shaking. The 1256 Medina event (MMI = IV) is likely related to volcanic activity. Smoke was seen from Medina and a lava flow approached the city. At present, lacking any further historical information and any field geologic investigations relating to the reported ground fissuring, the locations of the earthquakes that caused these reported shaking phenomena cannot be determined confidently. It may be reasonable to assume, however, that if the locations of ground disruption for the 1068 event (Khaybar and Tayma and presumably between these locations) approximate the epicentral region, this event was of tectonic origin as opposed to the apparent volcanic origin of the 1256 (MMI = IV) Medina event.

In contrast to the paucity of information related to historical earthquakes in western Saudi Arabia, Ambraseys and Melville (1983) have outlined a generally continuous record of moderate-sized earthquakes occurring in Yemen over the past 12 centuries. Most recently, the December 13, 1982 (Ms = 5.7) earthquake near Dhamar, North Yemen, caused considerable destruction and loss of life (Arya and others, 1985). The earthquake occurred in an area of active extensional tectonism characterized by horst-and-graben structure and Holocene basaltic vulcanism (Geukens, 1966).

The dearth of information concerning the historic and contemporary seismicity of the Arabian shield presently precludes any systematic seismotectonic analysis of the region. To construct seismic source zones for this region, therefore, we have imposed a hypothesis that relates any significant future earthquake activity in the shield to seismic reactivation of Precambrian faults. Thus, the source

zones conform to Precambrian tectonic provinces and regional Precambrian structural trends. The approach is justified, in part, by studies of intraplate earthquakes in the United States (for example, Hamilton, 1981) and worldwide (Sykes, 1978) which conclude that there is fairly clear evidence for larger intraplate earthquakes to be caused by reactivation of ancient, Precambrian faults or fault systems. Some support for applying this approach to source zones on the Arabian Shield is lent by microseismicity studies of Merghelani (1979) and Merghelani and others (1981). Merghelani notes concentrations of epicenters near structural lineaments of probable Precambrian origin, and near Precambrian faults such as the northeast-trending Ad Damm fault near Taif. Speculatively, there may be an association between shaking felt at Taif in 1270 and Mecca in 1481 (Poirier and Taher, 1980) and the Ad Damm fault that is in close proximity to both of these locations. Incidental support of the approach to source zones comes from recognition of the profound role played by Precambrian faults and fault systems in the development and disposition of the east Africa rift system (McConnell, 1967, 1972; Harpum, 1970). However, the fact that the Red Sea rift cuts across major, northeast Precambrian trends could perhaps be used as an argument against significant Tertiary structural control by Precambrian structure. At best, the Red Sea rift strikes parallel to a subordinate, relatively poorly developed north-northwest system of short Precambrian faults and structural lineaments.

The Najd fault system comprises the northeasternmost zone of the study area (figs. 2, 3). To the northwest, the Najd zone is terminated by zones of the Dead Sea rift and Red Sea rift. To the southeast, the Najd zone extends beneath Mesozoic sedimentary cover rock to include the terminous of the fault zone as depicted by Brown (1972). Included within the Najd zone are the historically reported shaking events near Medina, Kaybar, and Tayma (Poirier and Taher, 1980).

Southwest of the Najd fault system, the northeast-trending faults of the central Hijaz-Asir Precambrian tectonic province have been separated from the braided north- and north-northeast-trending faults of this province. The Ad Damm fault is a prominent feature of this northeast-trending zone.

In the southwestern portion of the Arabian Peninsula, the seismicity of the Yemen area is collected by a zone that is defined primarily by the regional exposure of the Yemen Trap Series volcanics. While not explicitly keyed to structure, the zone as drawn is thought to include the primary region of significant contemporary extensional tectonism in the southwestern part of the Arabian Peninsula. The northern boundary is of utmost importance to the city of Jizan, Saudi Arabia. Unfortunately, however, this boundary is poorly defined at present. Jizan has been included in the zone of relatively high seismic activity of North Yemen because of the January 11, 1941, earthquake (M_s = 5.8; Ambraseys and Melville, 1983) that occurred about 75 km east of Jizan near Rayih. The earthquake caused widespread damage in North Yemen although the earthquake was apparently only felt in Jizan.

EARTHQUAKE RECURRENCE MODEL

The worldwide earthquake catalog of the National Earthquake Information Service (NEIS), U.S. Geological Survey, served as the primary source for earthquake information in the region with entries cross-checked and additions made from other published seismicity studies in the region (Poirier and Taher,

1980; Ambraseys and Melville, 1983; Fairhead and Girdler, 1970; Sykes, 1970; Sykes and Landisman, 1964). Significantly more documentary work is required to ensure a complete historical catalogue.

Fairhead and Girdler (1970) concluded that earthquakes of $m_b > 5.0$ ($M_s = 4.8$) and $m_b > 4.8$ ($M_s = 4.5$) were well detected in the Red Sea and Gulf of Aden respectively since the early-mid 1960's. Our analysis corroborates their work and indicates 20 yrs of complete reporting for events $m_b > 4.5$; earthquakes smaller than $m_b = 4.5$ are not of interest in this study since they are not generally associated with damage to structures. Joint epicenter relocations by Fairhead and Girdler (1970) indicated that earthquakes occurring in the northern and central Red Sea between 1962-68 and having magnitudes $m_b > 4.1$, epicentral locations in the catalog were in error by no more than 0.20^o in either latitude or longitude. In the southern Red Sea-northern Ethiopian region, one relocated epicenter shifted 0.6^o in latitude. The remaining relocations, however, were less than 0.35^o. In the eastern Afar-Gulf of Aden region, while one relocated epicenter shifted 0.46^o in longitude, remaining relocations were less than 0.35^o. Our conclusion is that epicenter locations as reported in NEIS catalog (formerly the U.S. Coast and Geodetic Survey catalog) through 1984 are adequate for a regional investigation where seismic sources correspond to regional geologic provinces. Further investigations of individual epicenters would be required for a study dealing with local, seismically active faults.

Measures of earthquake size appear in the catalog as body-wave magnitude (m_b), surface-wave magnitude (M_s), local magnitude (M_L), and epicentral intensity (I_0). For statistical analysis of earthquake recurrence frequencies, the various measures of earthquake size were converted to M_s magnitudes. A least-squares regression fit to the catalog data gives the equation:

$$M_s = 1.36 \, m_b - 2.02$$

Similar fits to magnitude-intensity data of the catalog yield:

$$M_s = 0.6 I_0 + 0.85$$

Fits of M_L on I_0 give results identical to M_s on I_0 above although the few earthquakes having M_L measures are less than $M_L = 5.5$. Catalog M_L magnitudes were assumed equivalent to M_s magnitudes.

The approach assumes similar source properties for all earthquakes which is probably not strictly correct considering the different tectonic settings represented in the earthquake catalog. Ground-motion amplitudes and predominant periods of ground motion for various magnitude measures is likely to vary among the tectonic environments. However, significantly more seismological research throughout the region is required to conduct source-property studies that would substantiate this notion and to allow a proper treatment of magnitudes and attenuation throughout the region.

SEISMICITY PARAMETERS

Determination of constants a and b in the Richter relation of occurrence frequencies, $\log N = a - bM$, followed from a series of statistical tests of the earthquake data base. The seismic source zones were classified into oceanic rifting and continental divisions to investigate the possible existence of statistically significant differences in b-values for various tectonic settings

26

represented in the earthquake catalog. Oceanic-rifting zones were subdivided into areas of transform faults and areas not having known or inferred transforms. In the Red Sea and Gulf of Aden, earthquakes located generally within 30 km of a known or inferred transform fault or transform zone were assumed to be associated with transform faulting. Time of complete earthquake reporting was estimated for both oceanic and continental earthquake catalogs according to the methods described by Stepp (1973) and Weichert (1980). B-values of maximum likelihood fits to the entire catalogue data base and to subcatalogs are summarized in table 1.

TABLE 1.--B-value estimates using two maximum likelihood techniques

Tectonic category	Maximum likelihood methods	
	Fits to annual rates	Weichert (1980)
Oceanic		
a) Transform----------------	-0.92	-0.89
b) Nontransform-----------	-1.01	-1.04
Continental--------------------	-0.89	-1.02
Combined tectonic categories---	-1.00	-1.11

Bender (1983) has published curves showing 50-percent and 90-percent confidence regions for b-value fits to simulated seismicity data. As expected, when the numbers of earthquakes in a sample become smaller, the b- values have progressively larger confidence limits. For 40 earthquakes, about the number used in each tectonic category above, the 75-percentile and 25- percentile b-value estimates lie at about 1.15 times b, and 0.87 times b, respectively (derived from fig. 5 of Bender, 1983). On this basis, we concluded that the data are insufficient to prove that the different tectonic categories have b-values different from that of the fit to the combined data set. Accordingly, we adopted one of the two maximum likelihood fits to the combined data. We chose -1.00 obtained from the maximum likelihood fit to annual rates, because, although both techniques gave comparable values for predicted rates for modest-size earthquakes, the fit to annual rates results in rates about 50 percent higher for earthquakes in the magnitude 6.55 to 7.15 category. We decided to accept the more conservative value. However, because the hazard estimates are not critically sensitive to earthquake occurrence rates at high magnitudes, the choice of one over the other would not result in a significant difference in ground-motion values.

There are too few earthquakes to fit a-values for individual source zones or source-faults; hence, it is necessary to allocate the seismicity from a regional seismic activity rate into the constituent source zones and faults. Two optimal ways for statistically performing this allocation exist, maximum likelihood and minimum chi-squared procedures. For the maximum likelihood technique of allocation, the rates are allocated according to the total number of earthquakes observed in a zone. This count is taken for earthquakes above some magnitude for which the seismicity of the regional source zones are assumed to be complete.

Whereas the maximum likelihood technique is insensitive to the magnitudes of the earthquakes observed in a zone, the minimum chi-squared technique is not, giving somewhat higher allocations to zones in which higher magnitude events have occurred. Extensive testing with simulated data suggests that the minimum chi-squared technique may be superior to the maximum likelihood technique when independence of earthquake occurrences within a zone is not assured, and it is believed that the occurrence of a high-magnitude event inhibits the occurrence of subsequent lower magnitude events for the duration of the catalog. Furthermore, because of lower sensitivity to the occurrence of lower magnitude events, the minimum chi-squared technique may be the preferred technique when there is a considerable difference in the completeness times of the lower magnitude categories. The maximum likelihood technique, because it only depends on the number of earthquakes observed and not on their magnitude, overweights the contribution of small events.

In two cases, the appropriate allocation technique adopted depended on whether some a-priori estimate of a null hypothesis for seismicity was confirmed in the allocation. As stated in sections D and E below, this meant that for oceanic transform faults we assumed a-priori that the rate per unit length among all the transform faults should be equal and chose the allocation technique which gave a reasonable approximation to that assumption.

SEISMIC-RATE ALLOCATION SEQUENCE AND METHODS

Figure 7 schematically illustrates the various steps of the seismic rate allocation procedure. These steps, A through F, are outlined below.

Allocation	Method
A. Allocation of regional seismic activity rate into three tectonic categories of zones: oceanic nontransform zones, oceanic transform zones, continental zones.	Maximum likelihood.

Comment: Seismicity rates resulting from this allocation for magnitude-6.5 earthquakes are about 50 percent higher than rates from direct fits to the seismicity of the individual tectonic-categories.

B. Seismicity rate of oceanic, non-transform zones into northern and southern Red Sea zones and zones around Sheba Ridge in the Gulf of Aden.	Maximum likelihood.
C. Seismicity rate of oceanic, transform zones into overall rates for both the southern Red Sea and Gulf of Aden transforms.	Minimum chi-squared (unequal completeness for magnitudes below 5.5).

Comment: Direct allocation into individual transform fault zones at this stage would have reduced the Red Sea transform rates by a factor of 2 overall and would have produced rates inconsistent with our assumption of equal-rate-per-unit-fault-length.

D. Overall seismicity rate for Gulf of Aden transforms into individual transform faults.

Maximum likelihood (best conformance with equal-rate-per-unit-length assumption).

E. Overall seismicity rate for southern Red Sea transforms into individual transform faults.

Maximum likelihood (best conformance with our equal-rate-per-unit-length assumption).

F. Overall seismicity rate for the continental tectonic category into individual source zones.

Minimum chi-squared (unequal completeness).

Comment: Eight zones are assigned approximately the same rates under either maximum likelihood or minimum chi-squared allocation; four zones had allocated rates varying between 0.5 and 3 times the rate allocation from the maximum likelihood method.
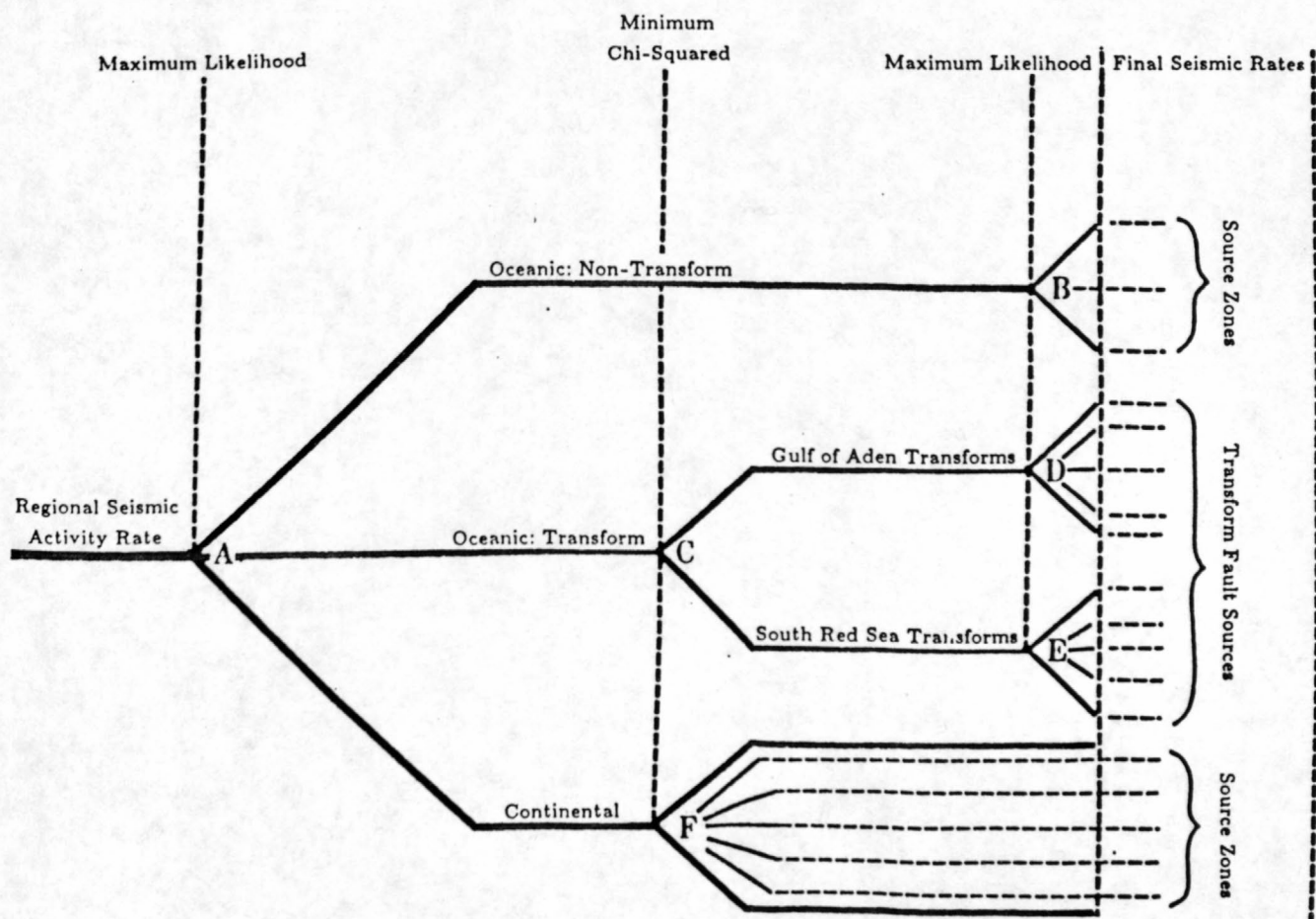
Figure 7.--*Allocation scheme of distributing regional seismic activity rate into contituent seismic source zone and faults. Steps labeled A through F correspond to descriptions of procedures in text.*

For each seismic source zone, an estimate of the maximum possible size of potential earthquakes is required to truncate the exponential frequency distribution. Due primarily to the lack of insight into distinctions in potential earthquake-source dimensions among many of the seismic source zones, maximum magnitudes were assigned to broad geologic categories of source zones and apply respectively to each seismic source zone comprising each category. The highest maximum magnitude (M_S=8.0) is assigned to the three segments of the Dead Sea transform and is based on the historical occurrence of an estimated M=8.0 on the northern segment (Ben-Menahem, 1981). Long fault lengths and historical occurrences of earthquakes having estimated magnitudes, $\geq$7.0 in the central and southern segments (Ben-Menahem, 1981), were the bases of assigning a maximum magnitude M_S=8.0 to these segments.

The maximum magnitude assigned to seismic source zones of the Red Sea and Gulf of Aden is M_S=6.5. Spreading ridge faults (located off of the ridge axes by 10 km) similarly are assigned M_S=6.5. This estimate is about one magnitude unit higher than the highest instrumentally determined magnitudes for earthquakes that could not be confidently associated with known or inferred transform faults. The corresponding m_b magnitude is about 6.25 and fits well with Solomon and Burr's (1979, fig. 1) nominal upper bound for spreading ridge-axis earthquakes on ridges with half-spreading rates of 0.6 cm/yr; the estimated half-rate of the Red Sea spreading ridge.

Oceanic transforms, on the other hand, were assigned a maximum magnitude of M_S=7.2. This estimate is based on the 1959 occurrence of an m_b=6.7 (M_S=7.1) earthquake on the Allula-Fartak transform in the Gulf of Aden (Sykes and Landisman, 1964). Because the remaining oceanic transforms in the Red Sea and Gulf of Aden are considerably shorter than the Allula-Fartak zone, this size event might be considered an overestimate of the maximum potential earthquake for these transforms. However, complicating any simple relation between transform length and earthquake size are observations by Burr and Solomon (1978) and Solomon and Burr (1979) that maximum moments, average fault width, and maximum moment sum increase with decreasing spreading velocities. From the empirical relations of Solomon and Burr between full spreading rate and moment for transform fault earthquakes, M_S=7.2 may underestimate the maximum magnitude earthquake by about 0.25 magnitude units. The spreading rate of the Red Sea rift would plot as a low extreme to their data base derived from worldwide examples of mature spreading-ridges. It is not clear that their empirical relations are valid for the poorly developed transform zones of the Red Sea spreading ridge.

The remaining zones of western Saudi Arabia, the Afar region of Ethiopa, and northeastern Egypt were also assigned maximum magnitudes of M_S=7.2. This value is about one magnitude unit higher than historically reported intensities (converted to Ms) or instrumentally recorded events in any of these regions.

The ground-motion estimates of this study are not critically sensitive to the choice of maximum magnitudes. Because of the low rate of seismic activity in the region, the mapped ground-motion values are well below the near-field ground motions produced by the chosen maximum magnitude earthquakes. Hence, the mapped ground motions are dominated by the more frequent occurrence of low- to

moderate-magnitude events. At longer return periods than addressed here, where ground motions approach those produced by the maximum magnitude earthquakes, choice of upper-bound earthquakes becomes a critical factor in determining ground-motion levels (Bender, 1984).

MODELING EARTHQUAKE EVENTS

Earthquakes are assumed to be equally likely throughout a zone and are modeled as point sources, or, as line sources of a length appropriate to magnitude/fault-rupture-length relations (Mark and Bonilla, 1977; Mark, 1977). Area-seismic-sources in this study are characterized by a low rate of earthquake activity. Hence, all earthquakes in these sources are modeled as point sources. Acceleration values in zones of low seismicity are correspondingly low at the return period addressed here, even when maximum magnitudes are high. Because these low accelerations affect large areas, the ratio of the isoseismal area to the size of the linear earthquake source is large, and a point source approximation can be justified (Bender, 1982, 1984b). However, in seismic source zones having relatively moderate-to-high rates of earthquake activity, modeling the larger earthquakes as linear ruptures is warranted and results in near-source ground-motion levels substantially higher than for point source models (Bender, 1982, 1984b). This is the case for the rift axes and transform faults of the study. A distinction was maintained in modeling earthquakes on the continental transform faults (Dead Sea Rift system) and the oceanic transforms (southern Red Sea and Gulf of Aden). Whereas the seismicity on continental transforms was modeled as a mixed-source type, that is, moderate-to-large earthquakes were modeled on faults and small earthquakes were modeled as point sources in an area around the faults, the oceanic transforms were modeled exclusively as fault sources. This modeling distinction was maintained, in part, because of tectonic dissimilarities between the two types of transforms, but also, because of extreme differences in size of the transform zones relative to the map scale being used here. Active fault deformation associated with large transform plate boundaries through heterogeneous continental crust can seldom be confined to a single, narrowly confined fault strand. The preceding discussions of the Dead Sea transform illustrate this point for that region. On the other hand, small offsets of young oceanic spreading ridges define only a very restrictad area where earthquakes related to rigid-plate transform faulting would be expected. On the regional scale of mapping being performed here, that area approaches a short linear source. Hence, representation of any area-source becomes unimportant to the ground-motion hazard estimate.

GROUND-MOTION ATTENUATION

A number of aspects of the gross crustal structure in western Saudi Arabia and the eastern Red Sea lead us to believe that attenuation of ground motions from earthquakes in this region may present a difficult problem. As there are no seismograph or strong-motion records from moderate-sized events, there is no direct data on strong-ground motion attenuation characteristics in western Saudi Arabia. Hence, an attenuation model developed outside of the region must be applied, but can only be justified if it can be demonstrated that the tectonic settings are generally similar. This becomes a difficult proposition in view of this uncertainty concerning the tectonic history, crustal composition and structure of the Red Sea rift.

Studies of attenuation of shear waves in the oceanic crust from a small number of earthquakes indicate very poor propagation (very low Q) for source-to-site paths crossing, or originating near, oceanic-spreading ridges, owing to the presence of high heat flow and partial melt immediately beneath the spreading ridge (Molnar and Oliver, 1969; Solomon, 1973). However, for some earthquakes on transform faults, source-to-site paths not crossing spreading ridge axes are characterized efficient transmission of shear waves (generally high Q) (Molnar and Oliver, 1969; Solomon, 1973). Observations from different transform faults may not be directly correlative, however, because of a growing recognition of the diversity of crustal structure and magmatic activity among oceanic transforms (Stewart, 1983). Efficient transmission of the Sn phase has been recognized across passive continental margins despite considerable lateral variations in crustal structure, composition, and thickness (Molnar and Oliver, 1969).

Of most importance in this study is the coastal region of Saudi Arabia where the largest metropolitan centers are located. At question is the attenuation characteristics along source-to-site paths from the eastern Red Sea to the coastal area where the propagation path does not cross the spreading-ridge axis, and from the Arabian shield area westward where the propagation path crosses abrupt lateral changes in crustal thickness and structure.

The Red Sea is generally characterized by high heat flow. Measured heat flow values in the axial trough of the southern Red Sea range as high as 5 HFU (1 $HFU=1 \times 10^{-6}$ cal/cm^2 sec) somewhat more than three times the worldwide mean, and apparently decrease rapidly beneath the shelf to about 2 HFU at the coast (Gettings and others, 1983). High heat flow typifies regions of the world known to have high attenuation (low Q); however, lithospheric strength has been suggested as correlating with low attenuation (high Q) (Oliver and Isacks, 1967; Molnar and Oliver, 1969). Interpretations of a seismic deep-refraction line across the southern Arabia shield, coastal plain, and shelf indicate a shallow mantle and a high-velocity crustal wedge beneath the shelf that thickens rapidly to 20 km beneath the coastal plain where the wedge is in abrupt vertical contact with nearly normal shield-type crustal structure (Mooney and others, 1985; Gettings and others, 1983) (fig. 8). The high-velocity wedge is inferred to be mafic crust emplaced through either ocean-floor spreading or massive diking in the early history of Red Sea rifting 20-25 m.y. B.P. It is not clear at present what effect this high velocity, presumably high strength, oceanic wedge would have on propagation paths of earthquake waves originating in the eastern Red Sea or along transform faults within this region of moderate-to-high heat flow.

Propagation paths east-to-west, from the shield area to the coastal plain, would seemingly best be described by an attenuation function incorporating low earthquake wave attenuation (high Q) typical of shield areas worldwide. However, some areas of the shield, north of the refraction line traverse, are characterized by generally north-south trending zones of extensive Tertiary and Holocene basaltic volcanism. High heat flow and partial melts at all crustal levels in these volcanic zones could substantially alter attenuation characteristics for propagation paths that cross them. The abrupt lateral and vertical change in crustal structure beneath thick unconsolidated sediments of the coastal plain raises further questions of possible focussing effects and (or) amplification of earthquake waves in the coastal plain region.
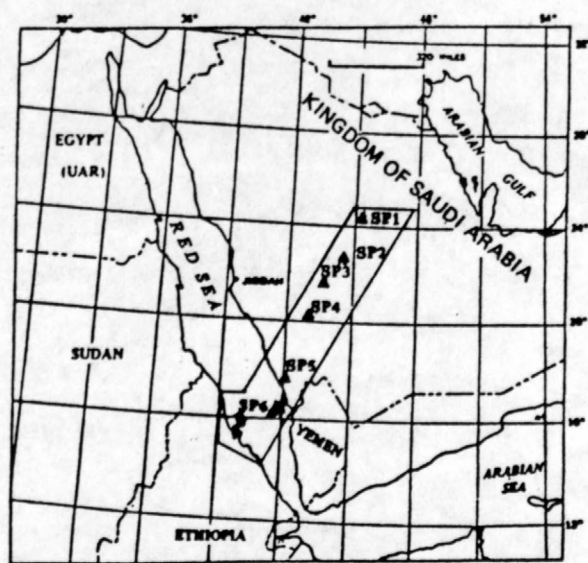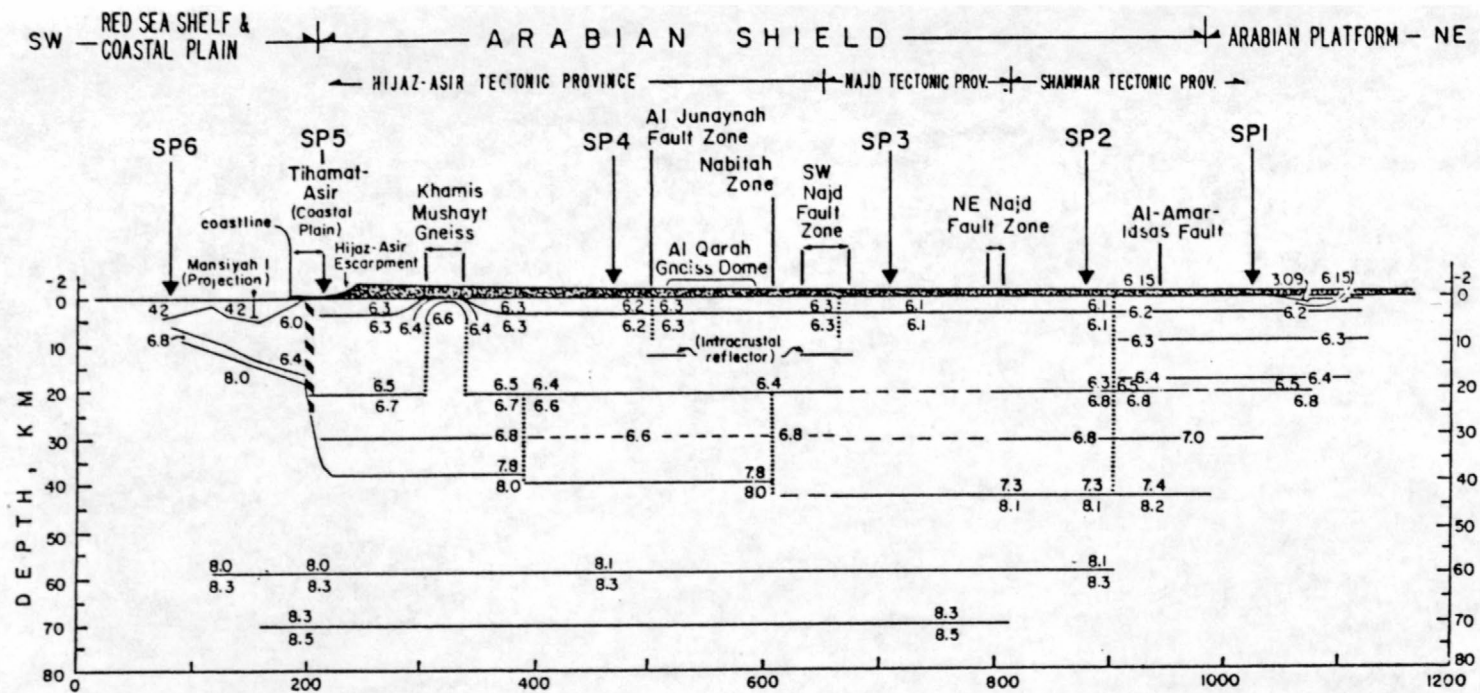
Figure 8.--*Interpreted velocity structure along the southwestern Saudi Arabian geophysical transect and seismic deep-refraction line (from Gettings and others, 1983).*
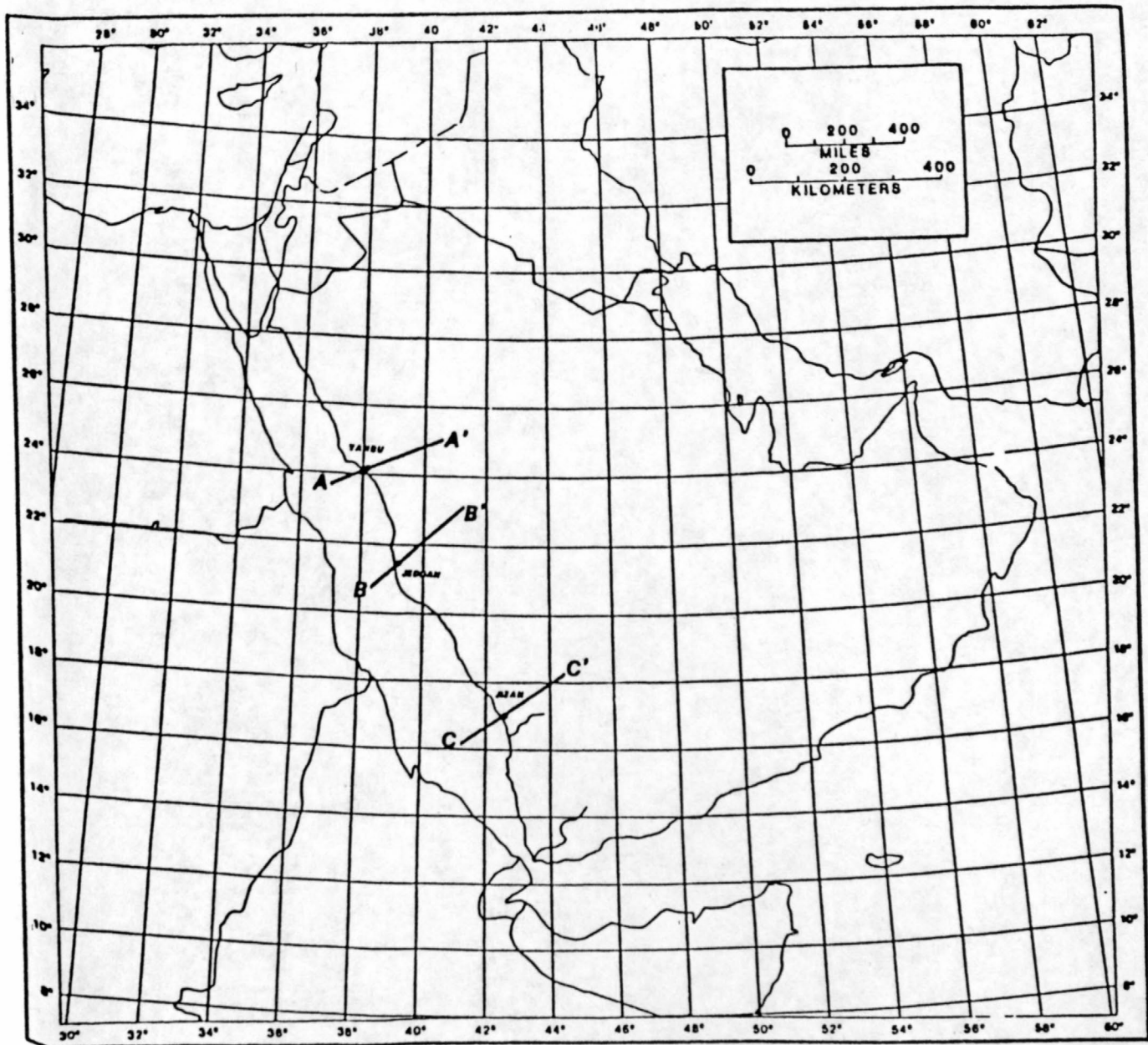
Figure 9.--*Index map showing the locations of three ground-motion profiles depicted in figures 10, 11, 20, and 21.*

In light of the uncertainties outlined above, we have investigated the consequences of modeling both a low-Q and high-Q attenuation function for all of the seismic source zones. We consider the ground motions derived from the high-Q attenuation function as generally upper bound values for the seismic source zones and seismic activity parameters of this study. There appears to be a good possibility that future research could justify the use of at least two attenuation functions; possibly a low-Q attenuation for zones of the Red Sea rift and a high-Q attenuation for the zones of the shield area. At present, however, pertinent data are too sparse to justify adding this complexity to the model.

Figures 10 and 11 are profiles of ground motion values calculated along lines extending from the Red Sea axial trough into the western Arabia shield (fig. 9). The figures summarize the range of ground motions calculated at Yanbu, Jeddah, and Jizan applying various assumptions in two attenuation models that pair peak horizontal ground acceleration and peak horizontal ground velocity. Whereas peak acceleration values usually occur at ground motion frequencies of around 5 Hz, peak velocity values generally occur around frequencies of 1-2 Hz. Therefore, velocity is generally a better measure of ground motion for applications concerned with long-period ground motions, such as earthquake effects on tall structures or high-rises located some distance from an earthquake source (see Steinbrugge, 1984, for discussion of some examples). Acceleration on the other hand, provides a better measure of ground motion at the higher frequencies experienced closer to the earthquake source and is generally better suited to considerations involved in low-rise construction.

The attenuation models used in this investigation are those of Nuttli and Herrmann (1984) and K. W. Campbell (written commun., 1984) that are derived using arithmetic mean peak values for the two horizontal components of strong ground motion. Nuttli and Herrmann's (1984) attenuation model is based on a semitheoretical approach that incorporates a small amount of strong-motion data from small earthquakes in the upper Mississippi Embayment and Atlantic coastal plain of the Eastern United States and theoretical relations between m_b and far-field accelerations and velocities in a high-Q region. The relations are valid for $4.5 \leq m_b \leq 7.4$. Because the NEIS catalog data was previously converted to M_s magnitudes for seismic rate determinations, a table of acceleration values as a function of m_b and epicentral distance was constructed using Nuttli and Herrmann's attenuation model. M_s magnitudes corresponding to Nuttli and Herrmann's m_b magnitudes were then determined using $M_s = 2.0 m_b - 5.6$ (Nuttli, 1983), which holds for $4.5 \leq m_b \leq 7.0$ (the range of magnitudes of significance in this study). Ground-motion values associated with catalog M_s values at various distances were then determined by interpolation in the table.

Nuttli and Herrmann's attenuation relations are developed for thick unconsolidated or stiff soil sites typical of the Mississippi Embayment and coastal plain regions of the Eastern United States; a surficial geologic setting grossly similar to the coastal region of western Saudi Arabia. Q at 1 Hz is taken as 1,500 in their relations. For $m_b \geq 4.5$, their relations for average mean peak horizontal acceleration (A_h, in cm/sec^2) and velocity (V_h, in cm/sec) are of the form:

$$\log A_h = A + 0.50\ m_b - 0.83 \log (R^2 + h^2)^{1/2} - BR \log e$$

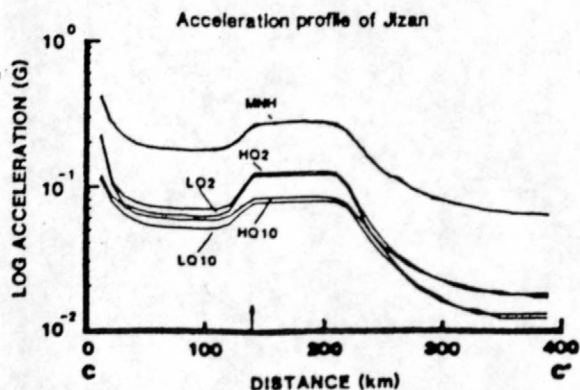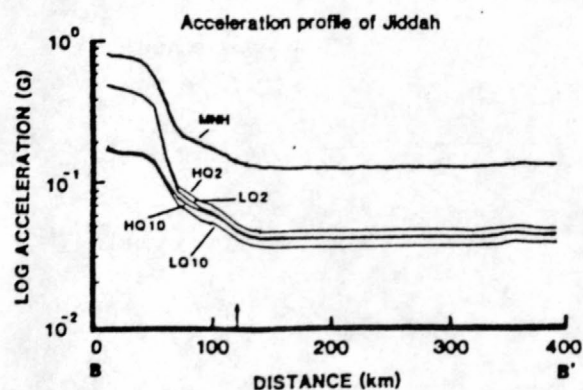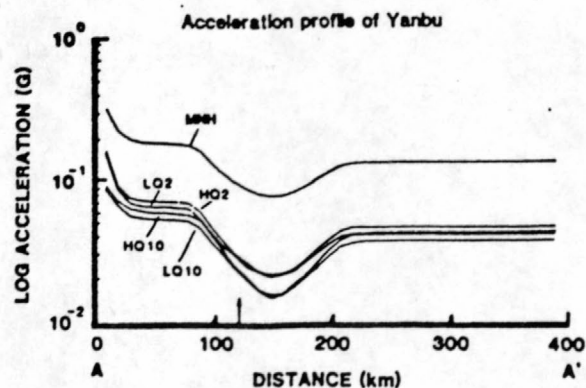$$\log V_h = C + 1.00\ m_b - 0.83 \log (R^2 + h^2)^{1/2} - DR \log e$$

36

Figure 10.--*Profiles of peak horizontal acceleration along transects shown in figure 9 applying various assumptions to two attenuation models. Vertical arrows indicate the locations of the cities of Yanbu, Jeddah, and Jizan along their respective profiles. MNH = modified Nuttli and Herrmann (1984) attenuation relation (focal depths have been held constant at 5 km). HQ2 and LQ2 = K.W. Campbell's (written commun., 1984) attenuation relation incorporating high-Q and low-Q values, respectively, assuming a 2-km depth to the top of the seismogenic zone (assumed top of crystalline basement). HQ10 and LQ10 = K.W. Campbell's (written commun., 1984) attenuation relation incorporating high-Q and low-Q values respectively assuming a 10-km depth to the top of the seismogenic zone.*

37

Velocity profile of Yanbu

Velocity profile of Jiddah
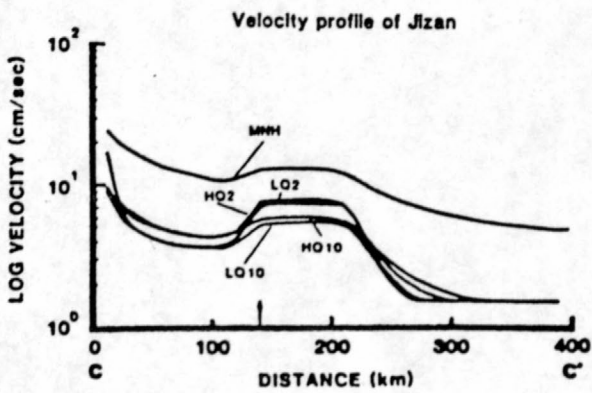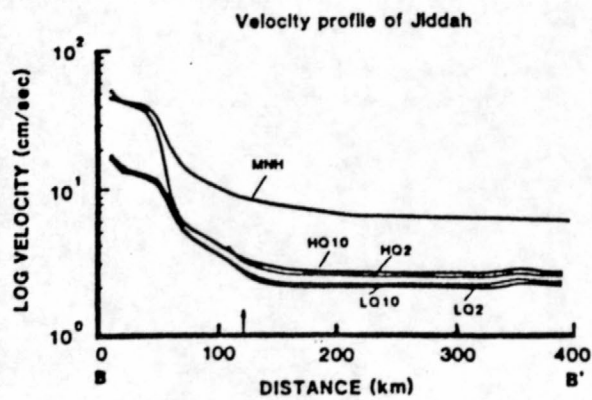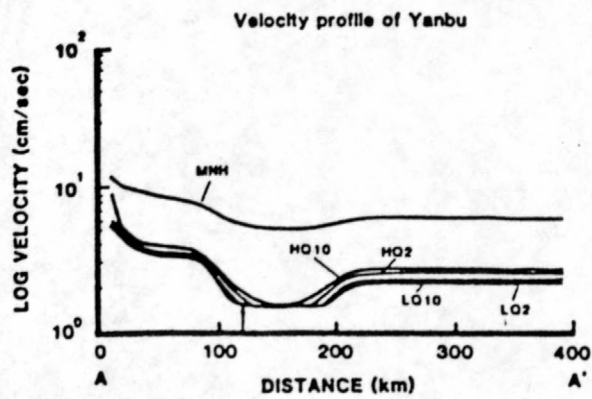
Velocity profile of Jizan

Figure 11.--*Profiles of peak horizontal velocity along transects shown in figure 9 applying various assumptions to two attenuation models. Labels are as in figure 10.*

where A and C are constants setting the level of the ground-motion curves for median values determined from available data for the Mississippi Valley, R is epicentral distance, h is minimum focal depth dependent on magnitude and given by $\log h_{(min)}=-1.730+0.456\ m_b$, for $m_b \geq 4.5$ (Nuttli, 1983), and B and D are equivalent to coefficients of an elastic attenuation in the Mississippi Valley region. The specific relations, given by Nuttli and Herrmann (1984) are:

$$\log A_h = 0.57+0.50m_b-0.83 \log (R^2+h^2)^{1/2}-0.00069R$$

$$\log V_h = -3.60+1.00m_b-0.83 \log (R^2+h^2)^{1/2}-0.00033R$$

In our application of these attenuation relations, focal depths (h) for earthquakes of all magnitudes have been held constant at 5 km. We did this for two reasons. First, Nuttli and Herrmann's (1984) attenuation relations are developed for an intraplate seismic zone that might have nucleation depths for large earthquakes down to a 40-km depth; the approximate base of the continental crust in the central United States. Such depths for earthquake nucleation in the Red Sea are unreasonable. Second, because of the lack of strong motion data and large uncertainty in characterizing the nature of ground motion attenuation along the Red Sea coast, we wanted an upper bound estimate of ground motion, given the seismic source zones and seismic activity rates of this study. The above treatment of the Nuttli and Herrmann (1984) attenuation relationships provides such an estimate.

The second set of attenuation models for mean peak horizontal acceleration and velocity were obtained from K. W. Campbell (written commun., 1984) and follow the form

$$\ln Y = a+bM-d \ln[R+c_1\exp(c_2M)]+\sum e_i k_i+\epsilon$$

where Y is the peak ground motion parameter, M is the magnitude (M_L for M<6.0 and determined by $M_L=2.241+0.621M_s$ from western U.S. data, K. W. Campbell, written commun., 1984; M_s for M$\geq$6.0), R is the shortest distance between the site and the seismogenic zone of rupture, k_i is a set of source and site variables and ϵ is a random error term (Campbell, 1981, 1982, 1983, 1984b). The specific relations used in this study for peak horizontal acceleration (PHA, in cm/sec^2) and velocity (PHV, in cm/sec) were (K. W. Campbell, written commun., 1984):

$$\ln PHA = -3.303+0.85M-1.25\ln[R+0.0872c^{0.678M}]+0.34F-0.0059R$$

$$\ln PHV = -1.584+1.18M-1.24\ln[R+0.0090c^{0.951M}]+0.49F+0.534Tanh(0.415H)-0.0059R$$

The relations are derived from worldwide strong motion data and incorporate California-type anelastic attenuation in which Q corresponds to 180 at 1 Hz (Joyner and Boore, 1981). Four profiles of ground motions (figs. 10 and 11) were generated using Campbell's relations incorporating high-Q, low-Q values, and 2- and 10-km depths to top of crystalline basement. Top of crystalline basement is taken to be the top of the seismogenic zone of rupture from which source-to-site distances are measured. This measure of distance is appropriate for moderate-to-large earthquakes where fault rupture may extend to the surface, since it is unlikely that the small stresses associated with rupture within the sedimentary section would contribute significant energy to surface ground motions (Campbell, 1984a, b).

39

Figures 12 and 13 illustrate the low and high extremes in the attenuation relations used in this study. Holding focal depth constant at 5 km in the high Q, Nuttli and Herrmann (1984) relations results in extremely high-ground motions for moderate to large earthquakes. We feel that ground-motion values derived from these curves are upper bound ground-motion estimates given the constituent source zone and fault models of this study.

The lower curves at any given magnitude (figs. 12, 13) were estimated from K. W. Campbell's (written commun., 1984) attenuation relations incorporating low-Q (high attenuation) and a 10-km depth to the top of the seismogenic zone (in this application, the top of crystalline basement). Curves for Campbell's attenuation relations assuming high-Q and a 10-km depth, and, both high- and low-Q at a 2-km depth, fall between the two sets of curves in figures 12 and 13.

Preferred Attenuation Model

Our preferred interpretation of ground-motion attenuation in coastal Saudi Arabia, based on presently available data, is given by Campbell's low-Q, 2-km-depth attenuation models for acceleration and velocity. Attenuation curves for these models are shown in figures 14 and 15. A low-Q model is preferred because of high-shallow crustal temperatures in and along the Red Sea rift. As previously mentioned, heat flow measurements across the southern Red Sea coast range as high as 5HFU in the axial trough to 2HFU at the coast (Gettings and others, 1983). In comparison, heat flow values for the Western United States, a region known to have high attenuation (low-Q), is generally characterized by values ≥ 1.5 HFU (Diment and others, 1975). In contrast, the Central and Eastern United States, known to be a region of low attenuation (high-Q), is characterized regionally by values ≤ 1.5 HFU (Diment an others, 1975).

GROUND-MOTION HAZARD MAPS

Figures 16 and 17 show the regional distribution of peak acceleration and velocity having a 0.90 (90 percent) probability of not being exceeded in 100 yrs for the preferred attenuation model. The highest predicted ground-motion values occur in extreme northwestern Saudi Arabia neighboring the Gulf of Aqaba. Accelerations up to 0.30 g and velocities up to 21 cm/sec are predicted and are governed by the fault-source model, the moderate rate of earthquake activity, and the potential for large earthquakes in the Gulf of Aqaba. The town of Haql, located on the northeastern shore of the gulf is included in this region of comparatively high-ground motion. Ground-motion values in coastal regions neighboring the Red Sea range from 0.05 g and 2 cm/sec at Yanbu, and 0.07 g and 4 cm/sec at Jeddah, to 0.13 g, 7 cm/sec at Jizan. The ground-motion values at Yanbu and Jeddah are governed by the seismic sources of the central Red Sea. The seismic source zones corresponding to the Precambrian shield tectonic provinces (figs. 2, 3) have a low rate of earthquake activity and result in relatively low-ground motions of around 0.04 g and 2 cm/sec over broad inland areas. The higher ground motions towards the coast at Yanbu and Jeddah are a result of distant ground motions from more frequent, larger earthquakes in the central Red Sea source zone. The ground motions predicted at Jizan, however, are not a result of seismic activity modeled in the central Red Sea, but rather, result from including Jizan in the zone of generally high seismicity in North Yemen. Whether or not it is appropriate to include Jizan in this seismic source zone cannot be confidently assessed until the seismotectonics of the southwest Arabian Peninsula are better understood.
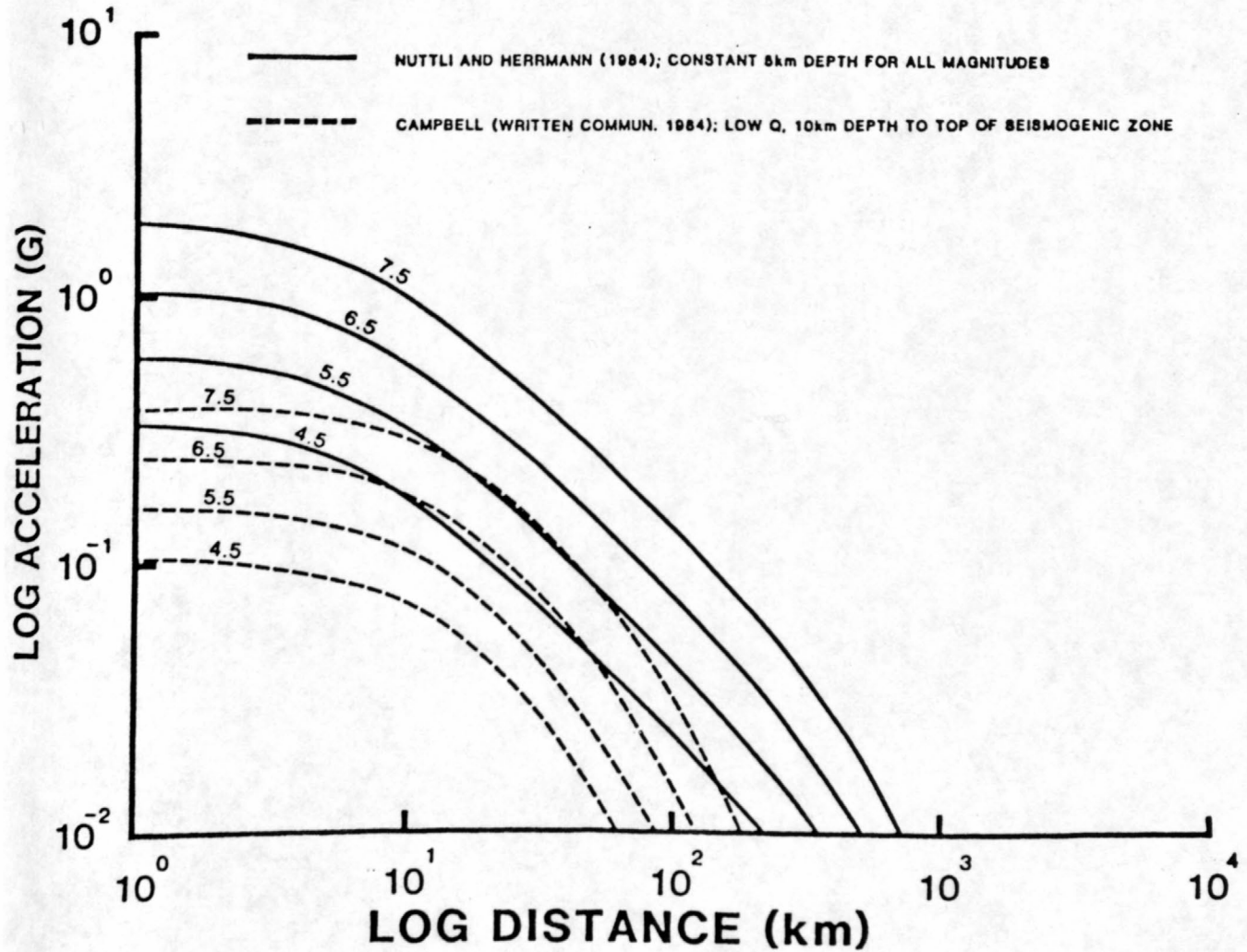
40

Figure 12.--*Acceleration attenuation curves illustrating the high and low extremes of attenuation relations investigated in the study. Magnitudes are M_S for Nuttli and Herrmann (1984) curves and M_S for $M \geq 6$, M_L for $M < 6$ for Campbell curves (written commun., 1984). See text for treatments of magnitude measures in the attenuation functions. Distance is epicentral distance for Nuttli and Herrmann curves and closest distance to the seismogenic zone of rupture for Campbell curves.*
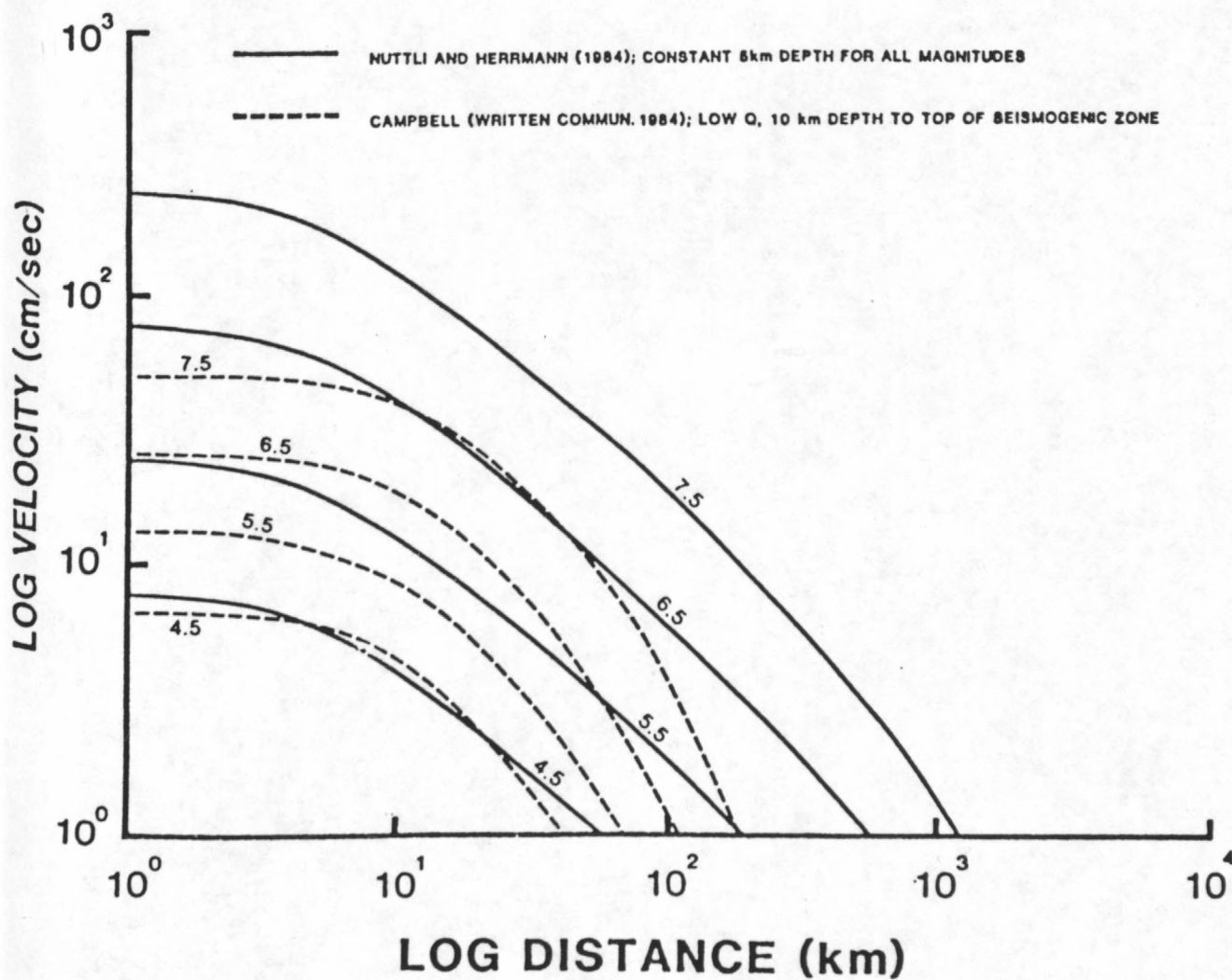
41

Figure 13.--*Velocity attenuation curves illustrating the high and low extremes of attenuation relations investigated in this study. Magnitudes and distance measures are as in figure 12.*
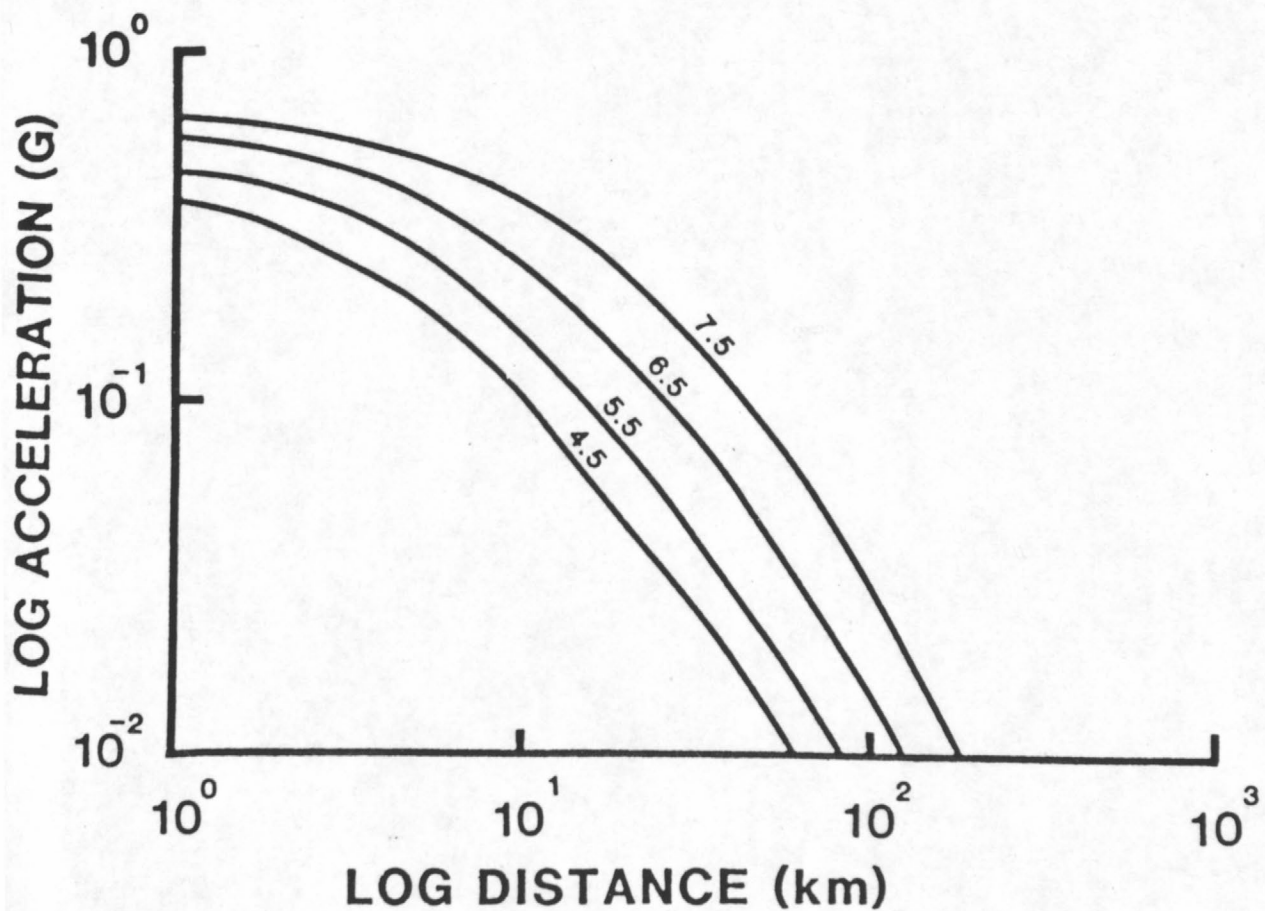
Figure 14.--*Acceleration attenuation curves for the preferred hazard model: K. W. Campbell (written commun., 1984), low-Q, 2-km depth to the top of the seismogenic zone. Magnitudes are M_S for $M \geq 6$ and M_L for $M < 6$. Distance is the shortest distance to the zone of seismogenic rupture.*
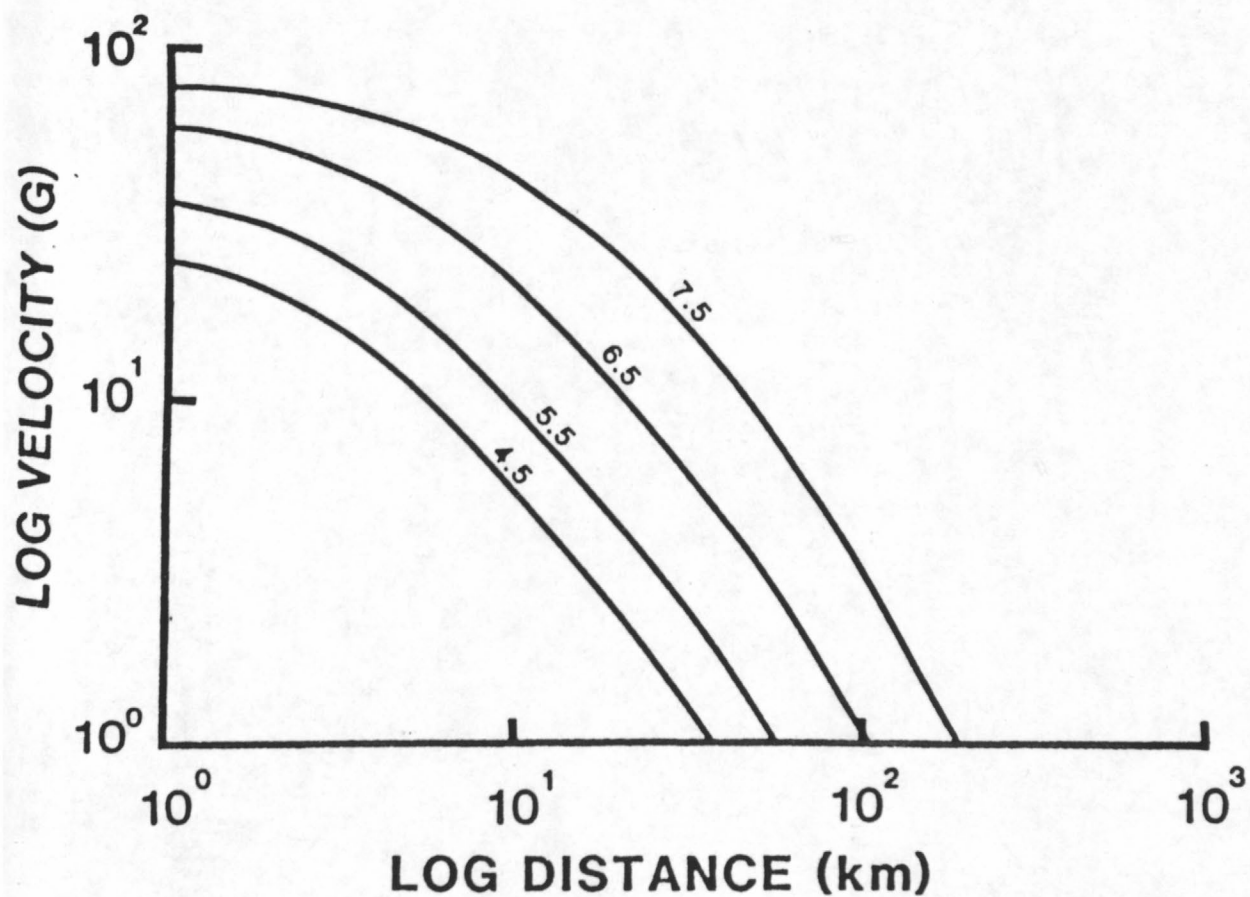
Figure 15.--*Velocity attenuation curves for the preferred hazard model: K. W. Campbell (written commun., 1984), low-Q, 2-km depth to the top of the seismogenic zone. Magnitude and distance measures are as in figure 14.*
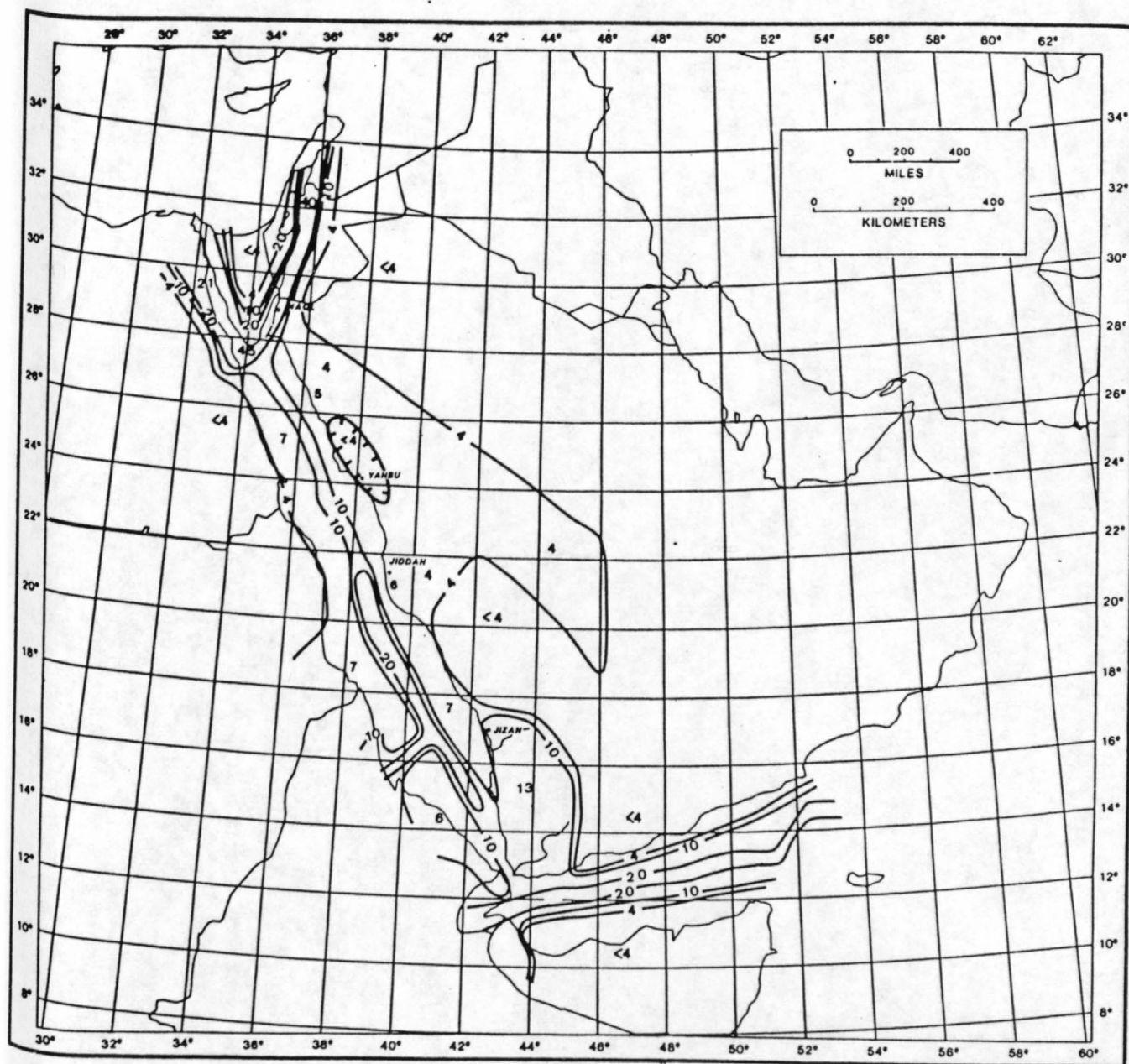
Figure 16.–*Peak horizontal acceleration having a 90-percent probability of not being exceeded in 100 yrs resulting from the preferred hazard model. Contours are in percent gravity.*
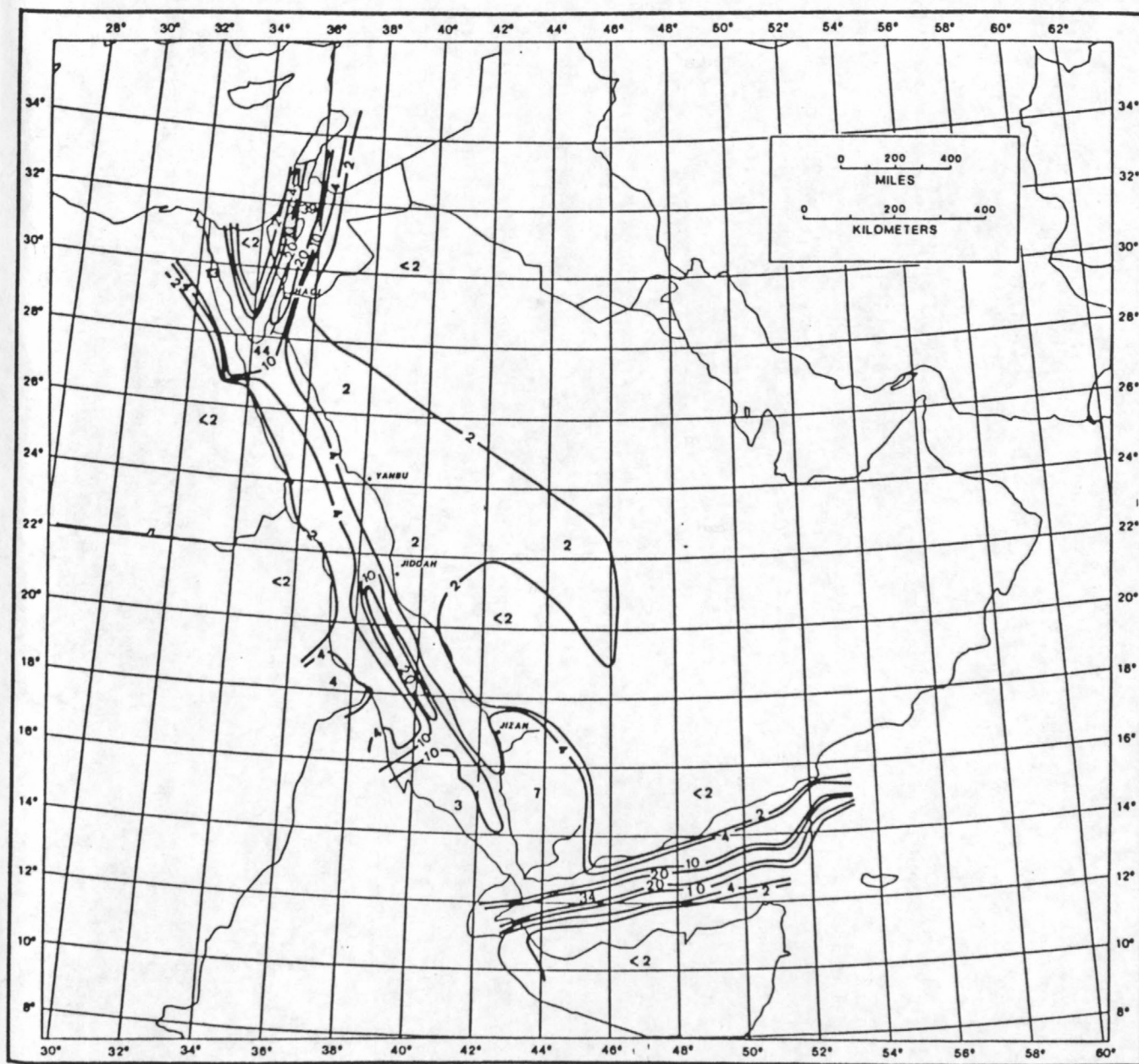
45

Figure 17.–*Peak horizontal velocity having a 90-percent probability of not being exceeded in 100 yrs resulting from the preferred hazard model. Contours are in centemeters per second.*
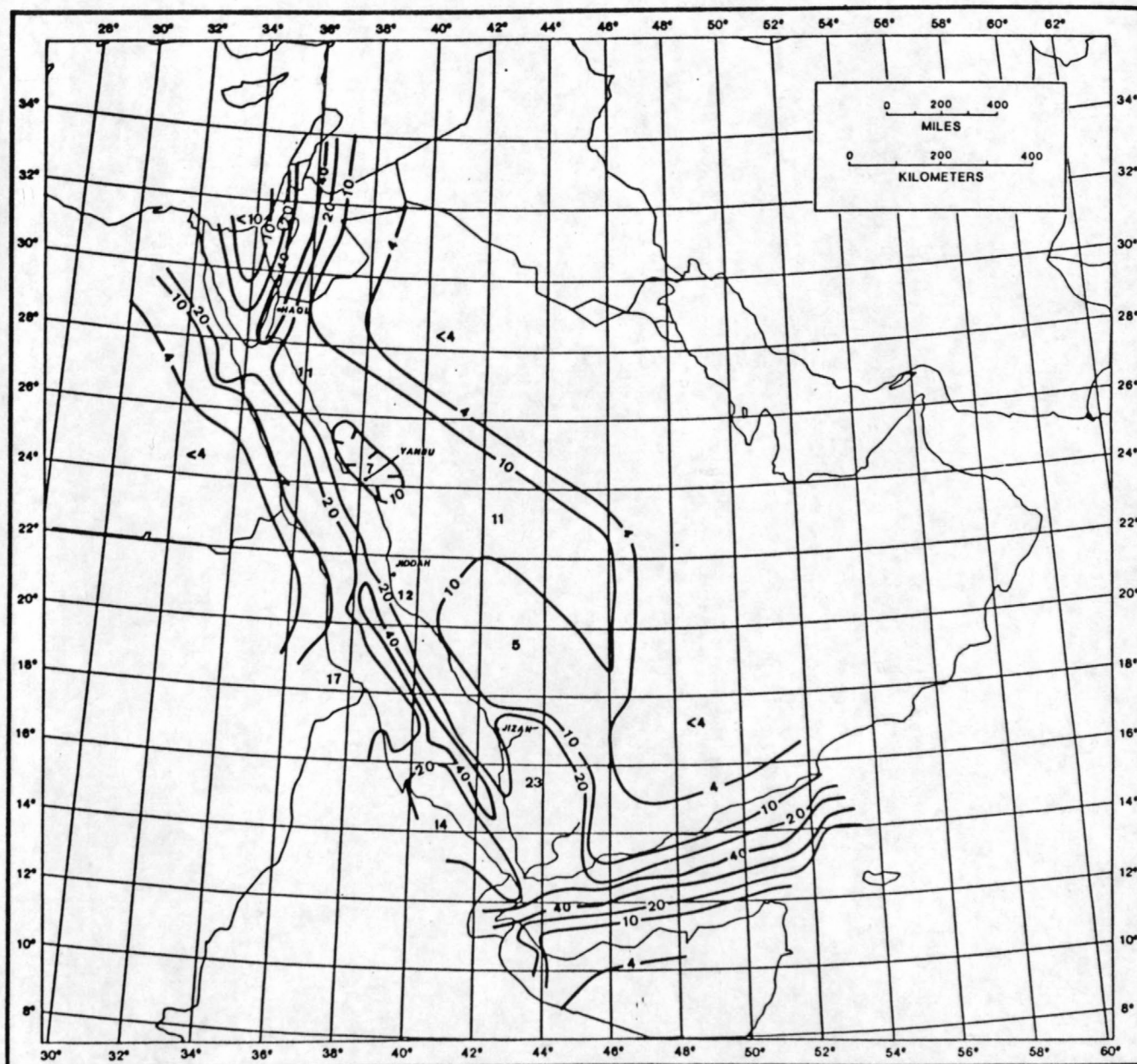
Figure 18.–*Peak horizontal acceleration having a 90-percent probability of not being exceeded in 100 yrs given by the upper-bound hazard model. Contours are in percent gravity.*
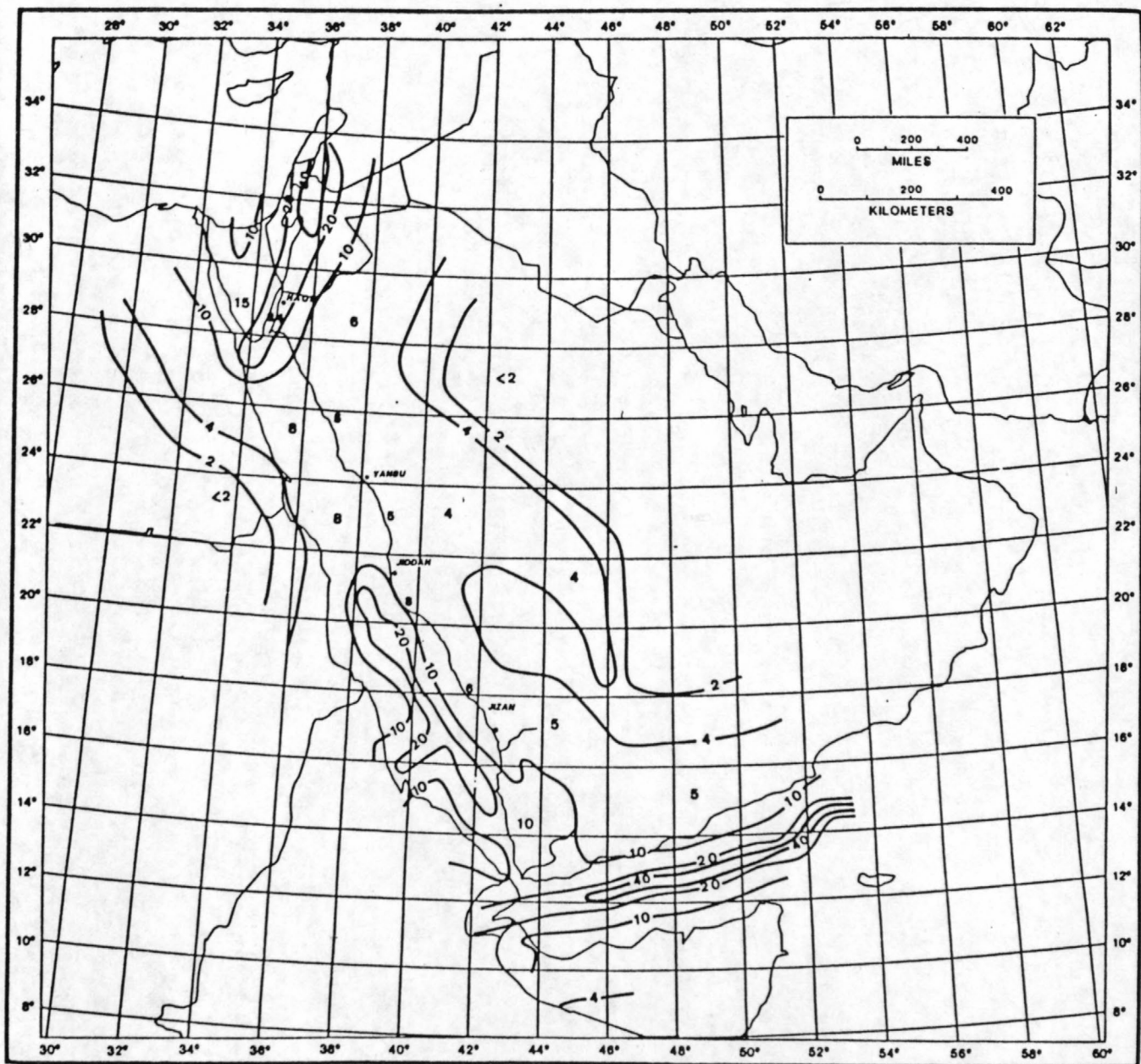
Figure 19.–*Peak horizontal velocity having a 90-percent probability of not being exceeded in 100 yrs given by the upper-bound hazard model. Contours are in centemeters per second.*

Figures 18 and 19 show probabilistic ground motions using the high-Q Nuttli and Herrmann (1984) relations. Regardless of what the actual ground- motion attenuation in western Saudi Arabia is (which could only be resolved through additional work beyond the scope of this report), our extreme treatment of the Nuttli and Herrmann (1984) ground-motion relations ensures conservative regional ground motion estimates for the seismic source zones and the earthquake recurrence model. Table 2 compares values at Haql, Yanbu, Jeddah, and Jizan for the preferred and upperbound models. The differences between the preferred and upperbound values of ground motion at any given location are large--the upperbound estimates being 40-50 percent larger at Haql to 150 percent larger at Yanbu. The larger differences at lower ground motions is attributable to the slower decrease of ground motion with distance in the Nuttli and Herrmann (1984) attenuation relations as compared to K. W. Campbell's (written commun., 1984) relations. While the ground motion differences between the preferred and upperbound models are large, the regional ground-motion values themselves are, in general, moderate to low as a result of the low rates of seismic activity in the Arabia shield area or, as along the coast, large distances from the modeled fault sources in the Red Sea rift.

Research has shown that statistical variability in ground-motion attenuation relations is a dominant source of uncertainty in estimated ground-motion values (McGuire and Shedlock, 1981; Bender, 1984). The standard deviation in log e acceleration appears to lie within a range of $0.35 \leq \sigma \leq 0.65$ and is generally assumed to hold for all magnitudes and distances of the relation (Bender, 1984). To illustrate the effect of this uncertainty on the estimated ground motions of this study, figures 20 and 21 compare ground motion levels along the profiles of figure 9 for the preferred and upperbound models with and without ground-motion attenuation variability. A standard deviation in log e (acceleration or velocity) of 0.5 is assumed. Results show that incorporating attenuation variability increases ground motions up to 60 percent for the highest levels of ground motion in the central Red Sea on the Jeddah profile. Increases in ground motion values for coastal and interior regions are considerably less. Table 2 summarizes the information for Haql, Yanbu, Jeddah, and Jizan.

TABLE 2.--Comparison of peak ground motion values
at Haql, Yanbu, Jeddah, and Jizan obtained
from the preferred and upperbound regional
hazard models. [Values in parentheses result
from assuming a standard deviation of 0.5 in
the attenuation relations.]

	Hazard model					
	Preferred		Upper bound		% Increase	
Location	Accel. (%g)	Vel. (cm/sec)	Accel. (%g)	Vel. (cm/sec)	Accel.	Vel.
Haql	30 (39)	21 (26)	43 (60)	31 (39)	43	48
Yanbu	4 (5)	2 (2)	10 (13)	5 (6)	150	150
Jeddah	6 (7)	3 (4)	14 (19)	7 (8)	133	133
Jizan	12 (15)	5 (6)	20 (26)	8 (10)	67	60
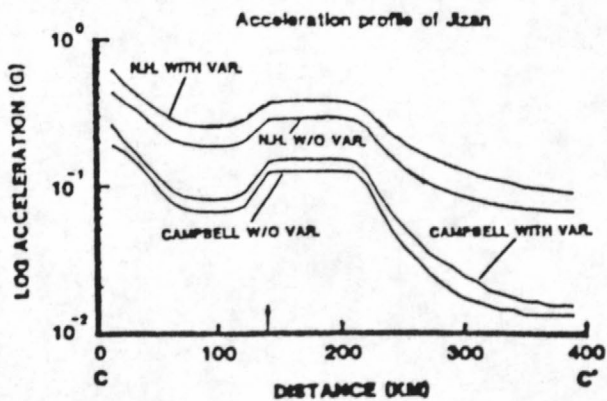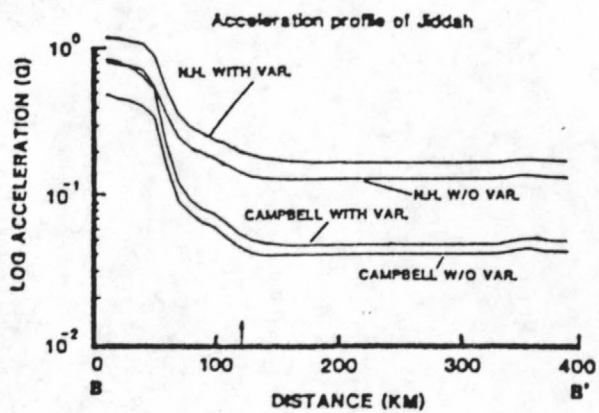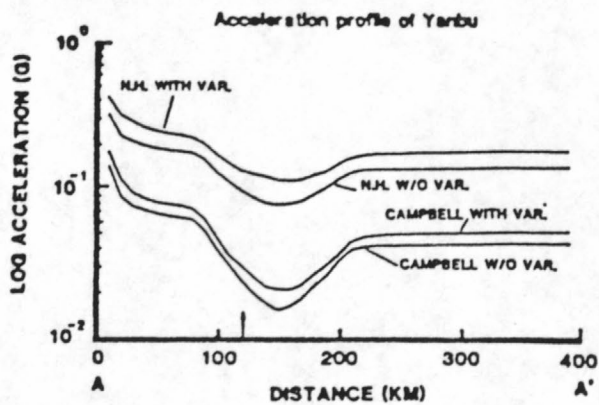
Figure 20.--*Profiles of peak horizontal acceleration along transects shown in figure 9 showing K. W. Campbell's (written commun., 1984) attenuation (model LQ2 in figure 10) and Nuttli and Herrmann's (1984) attenuation (model MNH on figure 10) with and without attenuation variability. Attenuation variability modeled as standard deviation 0.5 in $\log_e$ acceleration.*
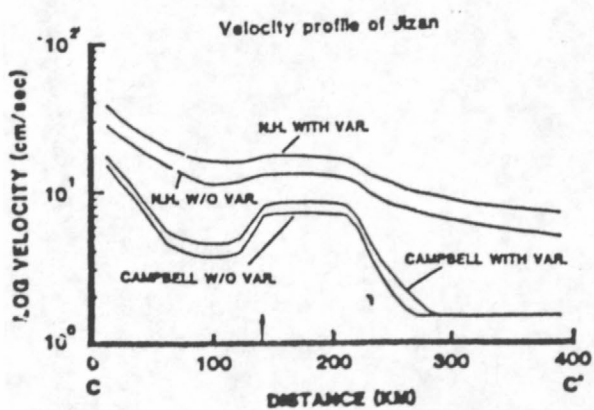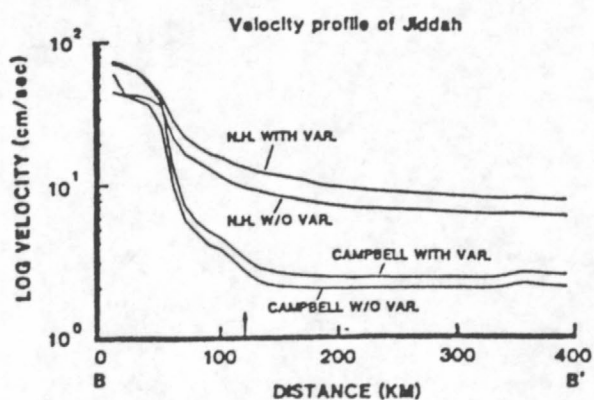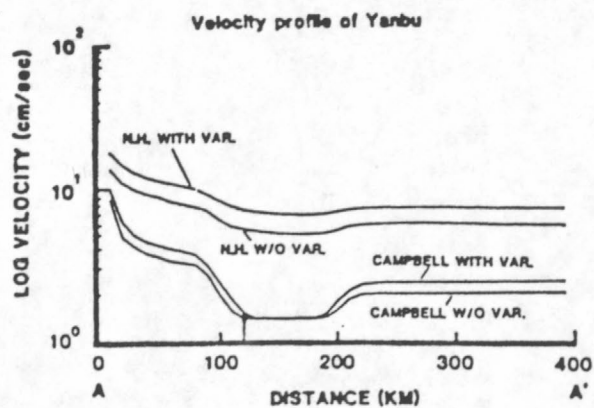
Figure 21.--*Profiles of peak horizontal velocity along transects of figure 9. Labels are as in figure 20. Attenuation variability modeled as standard deviation 0.5 in log_e velocity.*

51

DISCUSSION AND RECOMMENDATIONS

The approach to estimating the seismic hazard in the western Arabia Peninsula presented in this report was developed with full consideration of the limited data bases and scientific knowledge regarding the seismotectonics of the region. Indeed, the preferred and the upperbound hazard maps depict the consequences of models which depend more on scientific judgment than on well-established scientific fact. However, this work has served to highlight those questions that must be addressed to improve future hazard estimates. The hazard maps are submitted as an initial attempt to define the seismic hazard as reasonably as possible using existing data and information. However, an equally important aspect of this study is to identify areas of investigation of a somewhat broader scope that would serve to refine the overall understanding of the seismic hazard problem in western Saudi Arabia. In addition to outstanding questions discussed in the preceding sections of this report, three fruitful areas of further study can be identified: (1) historical and contemporary earthquake studies, (2) studies in contemporary tectonics and paleoseismic field investigations, and (3) investigations into secondary ground-failure hazards.

Refinement of the existing historical earthquake data base is likely to result from searches of primary Arabic sources. The search performed for this study was restricted to the English literature which, for noninstrumental earthquakes of record in the region, are secondary sources. Thorough searches of primary sources have considerably improved historical earthquake catalogs for areas of the Western United States (Oaks and Algermissen, 1984) in one case producing 50 percent more historic earthquakes than documented in existing catalogs of the southern basin-ranges region (Dubois and others, 1982). In the Eastern United States, a region of relatively low-seismic activity, it was the documented occurrence of large historical earthquakes in 1811-1812 (New Madrid earthquake sequence) and 1886 (Charleston, S.C.) that indicated a seismic hazard problem for this region thus providing impetus for scientific study. A correlative situation in western Saudi Arabia appears in the identification of strong earthquake shaking in the towns of Khaybar and Tayma in the year 1068 (estimated MMI = IX, Poirier and Taher, 1980). In terms of contemporary seismicity, the northwest Arabia peninsula appears virtually aseismic due in large part, perhaps, to a lack of local seismic monitoring. The historical accounts of strong shaking at Khaybar and Tayma are the first indications that a potentially serious, seismic hazard may exist in the area. Geologic field investigations of the reported ground disruptions between Khaybar and Tayma could serve to confirm the historical reports, and, if substantiated, could perhaps provide a preliminary epicentral area for the event. Geophysical studies and detailed microseismic monitoring could then provide detailed velocity structure and subsurface structure of the area along with accurate microseismic locations. The physical dimensions and geometry of the seismic source could thus be estimated and the potential local seismic hazard evaluated. This simplified investigation scenario follows the form of highly successful earthquake investigations in the Central and Eastern United States (McKeown and Pakiser, 1982; Bollinger and Wheeler, 1982).

Sufficient circumstantial evidence associating seismicity with the Ad Damm fault exists to warrant further earthquake-specific investigations for this fault. If this fault was found to be seismically active, it could very well dominate the earthquake ground-motion hazard at Taif and Mecca because of its

close proximity to both of these locations. Ground-motion hazard at Jeddah would result from both the generally far-field ground motions produced by the recurrence of earthquakes on the Ad Damm fault and those produced by earthquake sources of the central Red Sea Rift. At this point, all that can be confidently stated, is that if the Ad Damm fault is seismically active, it would be an important element to include in future hazard assessments of coastal Saudi Arabia.

While the presently known earthquake history of western Saudi Arabia resembles that of the Eastern United States, in that the rate of significant earthquake occurrences is apparently low, the recency of tectonic deformation of western Saudi Arabia corresponds to that of the Western United States. That is, Tertiary-Quaternary tectonics dominate the regional geologic structure of both areas. Because geomorphic/geologic studies of faults and fault scarps have found widespread success in identifying active faults in the Western United States tectonic setting, there is reason to believe that such investigations would similarly find success in western Saudi Arabia. Methods of investigation may not be directly transferable because of different regional climatic histories. Nevertheless, studies of landform degradation and climatic history could lead to paleoseismic, fault scarp investigation methods specific to the regions conterminous to the Red Sea. Relative and absolute age-datums necessary for distinguishing ages of faulting are already identifiable for the central and northern coastal regions in the form of raised terraces and coral reefs and interstratified Quaternary basalts (Whitney, 1982, unpub date). In one case, offset of a raised coral reef located about 45 km south of Jeddah has been suggested as due to late Pleistocene-Holocene age fault displacement (Pallister, 1982, unpub dta). However, fault studies up to the present have been only incidental to the primary goal of basic geologic mapping. Standard geologic mapping in the Western United States has proved to be far too insensitive to Quaternary tectonics and faulting to be useful in addressing geologically recent fault movements. Geologic maps are generally compiled without the required detail and without the proper emphasis on recent tectonics that is needed for careful evaluation of young fault movement. Important in seismic fault studies of coastal Saudi Arabia would be distinguishing tectonic, paleoseismic fault rupture from faulting due to salt diapirism, flowage, and solution. Tectonic faults extend to considerable crustal depths and are capable of storing sufficient stress to rupture in significant earthquakes. In contrast, diapiric and solutional faulting is restricted to the stratigraphic section and is generally not associated with earthquakes that produce damaging ground motions. Nonetheless, such faulting can result in surface displacement, thus posing a ground-displacement hazard to structures located on or near such faults.

The recommendation for locale-specific investigation may appear incongruous with the regional approach of this study. However, it is well known that hazard estimates can change dramatically for specific areas when causal seismogenic faults are identified and earthquake occurrence frequencies and maximum magnitudes are determined specifically for such faults. The consequence is that the hazard can be tied to specific faults, or classes of faults, rather than averaged over broad areas, thus resulting in a more accurate portrayal of a more local seismic hazard.

Secondary ground-failure hazards resulting from earthquakes such as surface rupture, liquefaction, and landsliding have not been topics of study in the current analysis. However, a thorough understanding of the earthquake hazard would include a knowledge of those areas susceptible to induced ground failure.

Sediments most susceptible to liquefaction are Holocene unconsolidated, cohesionless sands of delta, river channel, flood-plain or aeolian deposits, and uncompacted artificial fill, all located in areas having high-water tables (Youd and Perkins, 1978; Youd, 1984). Such conditions may exist at a number of locations along the Red Sea coastal plain. For example, ground-water levels near the wadi systems in the Jizan coastal plain are generally 10 m or shallower, with saturated alluvium of fluvial and aeolian origin extending to depths greater than 100 m (Müller and others, 1984). In Jeddah, a high-water table and development on unengineered fill and reclaimed land pose a potentially serious ground-failure hazard in the event of strong ground shaking.

Near-future progress towards a more complete understanding of the seismic hazard in the western Arabian peninsula is dependent upon a broad scope of interrelated geologic, seismologic, and geophysical investigations directed at specific "targets of opportunity." Historically reported ground disruptions associated with strong earthquake shaking, such as those reported at Tayma and Khaybar, provide such a target for scientific validation of the historical reports and scientific insights into possible earthquake sources of the region. With the experience and results of such an investigation, future studies could be structured in other areas of the western peninsula in full consideration of scientific methods of investigation that are likely to be applied successfully in the region.

ACKNOWLEDGEMENTS

DATA STORAGE

Field and laboratory data were not collected in the course of this investigations. Earthquake information was obtained from the National Earthquake Information Service, Golden, Colorado, as well as from published research as cited in the text.

MINERAL OCCURRENCE DOCUMENTATION SYSTEM (MODS)

No MODS entries were made as a result of the work described in this report.

REFERENCES CITED

Abdallah, A., Courtillott, V., Kasser, M., LePain, A., Lepine, J., Robineau, B., Ruegg, J., Tapponnier, P., and Tarantota, A., 1979, Relevance of Afar seismicity and volcanism to the mechanics of accreting plate boundaries: Nature, v. 282, p. 17-23.

Algermissen, S. T., and Perkins, D. M., 1976, A probabilistic estimate of maximum acceleration in rock in the contiguous United States: U.S. Geological Survey Open-File Report 76-416, 45 p.

Algermissen, S. T., Perkins, D. M., Thenhaus, P. C., Hanson, S. L., and Bender, B. L., 1982, Probabilistic estimates of maximum acceleration and velocity in the contiguous United States: U.S. Geological Survey Open-File Report 82-1033, 99 p.

Ambraseys, N. N., and Melville, C. P., 1983, Seismicity of Yemen: Nature, v. 3, no. 591, p. 321-323.

Arya, A. S., Srivastava, L. S., and Gupta, S. P., 1985, Survey of damages during the Dhamar earthquake of 13 December 1982 in the Yemen Arab Republic: Seismological Society of America Bulletin, v. 75, p. 597-610.

Barberi, F., Ferrara, G., Santacloce, R., Varet, J., 1975, Structural evolution of the Afar triple junction, in Piler, A. and Rosler, A., eds., Afar depression of Ethiopia: Inter-Union Commission on Geodynamics, Scientific Report 14, Verlagsbuchhandlung, Stuttgart, p. 38-54.

Barberi, F., and Varet, J., 1977, Volcanism of Afar--small-scale plate tectonics implications: Geological Society of America Bulletin, v. 88, no. 9, p. 1251-1266.

Bender, Bernice, 1982, Sensitivity analysis for seismic risk using a fault rupture model: U.S. Geological Survey Open-File Report 82-294, 75 p.

_____1983, Maximum likelihood estimation of b-values for magnitude grouped data: Seismological Society of America Bulletin, v. 73, p. 831-851.

_____1984a, Incorporating acceleration variability into seismic hazard analysis: Seismological Society of America Bulletin, v. 74, p. 1451-1462.

_____1984b, Seismic hazard estimation using a finite fault rupture model: Seismological Society of America Bulletin, v. 74, p. 1899-1923.

Ben-Menahem, Ari, 1981, Variation of slip and creep along the Levant Rift over the past 4500 years, in Freund, R., ed., The Dead Sea Rift--International Symposium on the Dead Sea Rift, Jerusalem, Sept. 10-20, 1979: Tectonophysics, v. 80, no. 1-4, (Special issue), p. 183-197.

Ben-Menahem, Ari, and Aboodi, Ezra, 1971, Tectonic patterns in the northern Red Sea region: Journal of Geophysical Research, v. 76, no. 11, p. 2674- 2689.

_____1981, Micro- and macroseismicity of the Dead Sea Rift and off-coast eastern Mediterranean, in Fruend, R., ed., The Dead Sea Rift-- International Symposium on the Dead Sea Rift, Jerusalem, Sept. 10-20, 1979: Tectonophysics, v. 80, no. 1-4 (Special issue), p. 199-233.

Ben-Menahem, A., Almagor, G., and Garfunkel, Z., 1981, Sediments and structure of the Gulf of Elat (Aqaba)-northern Red Sea: Sedimentary Geology, v. 23, p. 239-267.

Blank, H. R. Jr., 1977, Aeromagnetic and geologic study of the tertiary dikes and related structures on the Arabian margin of the Red Sea, in Red Sea research 1970-1975: Saudi Arabian Directorate General of Mineral Resources Bulletin 22, p. G1-G18.

Bohannon, R. G., 1985, A possible solution to the Afar-Yemen overlap problem encountered in tectonic reconstructions: unpublished manuscript.

Bollinger, G. A., and Wheeler, R. L., 1982, The Giles County, Virginia, seismogenic zone--seismological results and geological interpretations: U.S. Geological Survey Open-File Report 82-585, 136 p.

Brown, G. F., 1972, Tectonic map of the Arabian Peninsula: Saudi Arabian Directorate General of Mineral Resources Arabian Peninsula Map AP-2 scale 1:4,000,000.

Burr, N. C., and Solomon, S. C., 1978, The relationship of source parameters of oceanic transform earthquakes to plate velocity and transform length: Journal of Geophysical Research, v. 83, p. 1193-1205.

Campbell, K. W., 1981, Near-source attenuation of peak horizontal acceleration: Seismological Society of America Bulletin, v. 71, p. 2039-2070.

_____1982, Near-source scaling characteristics of peak horizontal acceleration for moderate-to-large earthquakes, in Boatwright, John, ed. and organizer, Proceedings of Conference XVI, The dynamic characteristics of faulting as inferred from recordings of strong ground motion: U.S. Geological Survey Open-File Report 82-591, v. 1. p. 120-184.

_____1983, The effects of site characteristics on near-source recordings of strong ground motion, in Hays, W. W., ed., Proceedings of Conference XXII, A workshop on site specific effects of soil and rock on ground motion and the implications for earthquake-resistant design: U.S. Geological Survey Open-File Report 84-845, p. 280-309.

_____1984a, The selection and development of strong motion scaling relationships for seismic hazard studies, in Williams, M. E., ed., Proceedings of the Geological and Hydrologic Hazards Training Program: U.S. Geological Survey Open-File Report 84-760, p. 28-82.

_____1984b, Near-source attenuation of strong ground motion for moderate to large earthquakes--an update and suggested application of the Wasatch fault zone of north-central Utah, in Hays, W. W., and Gori, P. l., eds., Proceedings of Conference XXVI, a workshop on evaluation of regional and urban earthquake hazards and risk in Utah: U.S. Geological Survey Open-File Report 84-763, p. 483-499.

Cochran, J. R., 1981, The Gulf of Aden--Structure and evolution of a young ocean basin and continental margin: Journal of Geophysical Research, v. 86, no. B1, p. 263-287.

_____1982, The magnetic quiet zone in the eastern Gulf of Aden--Implications for the early development of the continental margin: Geophysical Journal of the Royal Astronomical Society, v. 68, no. 2, p. 171-201.

_____1983, A model for the development of the Red Sea: American Association Petroleum Geologists Bulletin, v. 67, no. 1., p. 41-69.

Coleman, R. G., 1973, Geologic map of the Red Sea, in Red Sea Research 1970-1975: Saudi Arabian Directorate General of Mineral Resources Bulletin 22, pl. 1.

_____1977, Geologic background of the Red Sea, in Red Sea Research, 1970- 1975: Saudi Arabian Directorate General of Mineral Resources Bulletin 22, p. C1-C9.

Cornell, C. A., 1968, Engineering seismic risk analysis: Seismological Society of America Bulletin, v. 58, p. 1583-1606.

Crowell, J. C., 1974, Origin of late Cenozoic basins in southern California, in Dickinson, W. R., ed., Tectonics and sedimentation: Society of Economic Paleontologists and Mineralogists Special Paper 22, p. 190-204.

Diment, W. H., Urban, T. C., Sass, J. H., Marshall, B. U., Munroe, R. J., and Lachenbruch, A. H., 1975, Temperatures and heat contents based on conductive transport of heat, in White, O. E , and Williams, D. L., eds., Assessment of geothermal resources of the United States--1975: U.S. Geological Survey Circular 726, p. 84-103.

Drake, C. L., and Girdler, R. W., 1964, A geophysical study of the Red Sea: Geophysical Journal, v. 8, p. 473-495.

Dubois, S. M., Sbar, M. L., and Nowak, T. A., 1982, Historical seismicity in Arizona: U.S. Nuclear Regulatory Commission Report NUREG/CR-2577, 199 p.

Eyal, M., Eyal, Y., Bartov, Y., and Steinitz, G., 1981, The tectonic development of the western margin of the Gulf of Elat (Aqaba) Rift, in Freund, R., ed., The Dead Sea Rift--International Symposium on the Dead Sea Rift, Jerusalem, Sept. 10-20, 1979: Tectonophysics, v. 80, no. 1-4 (Special issue), p. 39-66.

Fairhead, J. D., and Girdler, R. W., 1970, The seismicity of the Red Sea, Gulf of Aden and Afar triangle: Philosophical Transactions of the Royal Society of London, v. 267, p. 49-74.

Forsyth, D., and Rowlett, H., 1979, Microearthquakes and recent faulting at the intersection of the Vema fracture zone and the mid-Atlantic ridge [abs.]: EOS, Transactions of the American Geophysical Union, v. 60, p. 376.

Francis, T. J. G., Porter, I. T., and Lilwall, R. C., 1978, Microearthquakes near the eastern end of St. Paul's fracture zone: Geophysical Journal of the Royal Astronomical Society, v. 53, p. 201-217.

Frazier, S. B., 1970, Adjacent structures of Ethiopia that portion of the Red Sea coast including Dahlah Kebir Island and the Gulf of Zula: Philosophical Transactions of the Royal Society of London, v. 267, p. 131-141.

Garfunkel, Zvi, 1981, Internal structure of the Dead Sea leaky transform (rift) in relation to plate kinematics, in Freund, R., ed., The Dead Sea Rift--International Symposium on the Dead Sea Rift, Jerusalem, Sept. 10-20, 1979: Tectonophysics, v. 80, no. 1-4 (Special issue), p. 81-108.

Garfunkel, Z., and Bartov, Y., 1977, The tectonics of the Suez rift: Israel Geological Survey Bulletin 71, 44 p.

Garfunkel, Z., Zak, I., and Freund, R., 1981, Active faulting in the Dead Sea rift, in Freund, R., ed., The Dead Sea Rift--International Symposium on the Dead Sea Rift, Jerusalem, Sept. 10-20, 1979: Tectonophysics, v. 80, no. 1-4 (Special issue), p. 1-26.

Gettings, M. E., 1977, Delineation of the continental margin in the southern Red Sea region from new gravity evidence, in Red Sea research 1970-1975: Saudi Arabian Directorate General of Mineral Resources Bulletin 22, p. K1-K11.

Gettings, M. E., Blank, H. R., Mooney, W. D., and Healy, J. H., 1983, Crustal structure of southwestern Saudi Arabia: Saudi Arabian Deputy Ministry for Mineral Resources Open-File Report USGS-OF-03-59, 51 p. Also, 1983, U.S. Geological Survey Open-File Report 83-638.

Geukens, F., 1966, Geology of the Arabian Peninsula--Yemen [translated from French by S. D. Bowers]: U.S. Geological Survey Professional Paper 560- B, 23 p.

Girdler, R. W., 1970, An aeromagnetic survey of the junction of the Red Sea, Gulf of Aden and Ethiopian rifts--A preliminary report: Philosophical Transactions of the Royal Society of London, v. 267, p. 359-368.

Girdler, R. W., and Styles, P., 1974, Two stage Red Sea floor spreading: Nature, v. 247, p. 7-11.

Gouin, P., 1970, Seismic and gravity data from Afar in relation to surrounding areas: Philosophical Transactions of the Royal Society of London, v. 267, p. 339-358.

_____1979, Earthquake history of Ethiopia and the horn of Africa: International Development Research Center, Ottawa, Canada, IDRC-118e, 259 p.

Gouin, P., and Mohr, P. A., 1964, Gravity traverses in Ethiopia: Bulletin of the Geophysical Observatory, v. 3, no. 2, p. 185-239.

Greenwood, W. R., Anderson, R. E., Fleck, R. J., and Roberts, R. J., 1980, Precambrian geologic history and plate tectonic evolution of the Arabian shield: Saudi Arabian Directorate General of Mineral Resources Bulletin 24, 35 p.

Gutenberg, B., and Richter, C. F., 1942, Earthquake magnitude, intensity, energy and acceleration: Seismological Society of America Bulletin, v. 32, p. 163-191.

_____1954, Seismicity of the earth [2nd ed.]: Princeton, N.J., Princeton University Press, 310 p.

Hall, S. A., 1980, A total intensity magnetic anomaly map of the Red Sea and its interpretation: U.S. Geological Survey Open-File Report 80-131, 271 p.

Hall, S. A., Andreasen, G. E., and Girdler, R. W., 1977, Total-intensity magnetic anomaly map of the Red Sea and adjacent coastal areas--A description and preliminary interpretation, in Red Sea research 1970-1975: Saudi Arabian Directorate General of Mineral Resources Bulletin 22, p. F1-F15.

Hamilton, R. M., 1981, Geologic origin of eastern U.S. seismicity, in Beavers, J. E., ed., Earthquakes and earthquake engineering--The Eastern United States, v. 1: Ann Arbor Science Inc., p. 3-24.

Harpum, J. R., 1970, Summary of the geology of Tanzania, [Chap.] V; Structure and geotectonics of the precambrian: Dodoma, Tanzania, Mineral Resources Division, 58 p.

Heirtzler, J. R., Dickson, G. O., Herron, E. M., Pitman, W. C., III, and LePichon, X., 1968, Marine magnetic anomalies, Geomagnetic reversals, and motions of the ocean floor and continents: Journal of Geophysical Research, v. 73, p. 2119-2136.

Joyner, W. B., and Boore, D. M., 1981, Peak horizontal acceleration and velocity from strong-motion records including records from the 1979 Imperial Valley, California, earthquake: Seismological Society of America Bulletin, v. 71, p. 2011-2038.

Juch, D., 1975, Geology of the southeastern escarpment of Ethiopia between 30° and 42° longitude east, in Pilger, A., and Risler, A., eds., Afar depression of Ethiopia: Inter-Union Commission on Geodynamics, Scientific Report no. 14, Verlagsbuchhandlung, Stuttgart, p. 310-315.

Kronberg, P., Schönfeld, M., Günther, R., and Tsombos, P., 1975, Tectonic relations of the Afar region and adjacent areas, in Pilger, A., and Risler, A., eds., Afar depression of Ethiopia: Inter-Union Commission on Geodynamics, Scientific report 14, Verlagsbuchhnadlung, Stuttgart, p. 19-27, 2 pls., scale 1:1,000,000.

Langer C. J., and Merghelani, H. M., 1983, Aftershocks of the Yemen earthquake of December 13, 1982--A detailed study from locally recorded data [abs.]: Earthquake Notes, v. 54, p. 20.

Laughton, A. S., 1966, The Gulf of Aden: Philosophical Transactions of the Royal Society of London, v. 259, ser. A. p. 150-171.

Laughton, A. S., Whitmarsh, R. B., and Jones, M. T., 1970, The evolution of the Gulf of Aden: Philosophical Transactions of the Royal Society of London, v. 267, p. 227-266.

LePichon, X., and Francheteau, J., 1978, A plate-tectonic analysis of the Red Sea-Gulf of Aden area, in Oren, O. H., ed., Structure and tectonics of the eastern Mediterranean: Tectonophysics, v. 46, p. 369-406.

LePichon, X., and Sibuet, J. C., 1981, Passive margins--A model of formation: Journal of Geophysical Research, v. 86, p. 3708-3720.

Mark, R. K., 1977, Application of linear statistical models of earthquake magnitude versus fault length in estimating maximum expectable earthquakes: Geology, v. 5, p. 464-466.

Mark, R. K., and Bonilla, M. G., 1977, Regression analysis of earthquake magnitude and surface fault length using the 1970 data of Bonilla and Buchanan: U.S. Geological Survey Open-File Report 77-614, 9 p.

McConnell, R. B., 1967, The east African rift system: Nature, v. 215, p. 578-581.

_____1972, Geological development of the rift system of eastern Africa: Geological Society of America Bulletin, v. 83, p. 2549-2572.

McGuire, R. K., and Shedlock, K. M., 1981, Statistical uncertainties in seismic hazard evaluations in the United States: Seismological Society of America Bulletin, v. 71, no. 4, p. 1287-1308.

McKenzie, D. P., Davies, D., and Molnar, P., 1970, Plate tectonics of the Red Sea and East Africa: Nature, v. 226, p. 243-248.

McKeown, F. A., and Pakiser, L. C., 1982, Investigations of the New Madrid, Missouri, earthquake region: U.S. Geological Survey Professional Paper 1236, 201 p.

Merghelani, H. M., 1979, Seismicity of the Tihamat-Asir region, Kingdom of Saudi Arabia: U.S. Geological Survey Saudi Arabian Project Report 261, 20 p. Also, 1979, U.S. Geological Survey Open-File Report 79-1191.

_____1981, Seismicity of the Yanbu region, Kingdom of Saudi Arabia: U.S. Geological Survey Saudi Arabian Project Report 371, Technical Record 16, 32 p. (unpublished data)

Merghelani, H. M., Kinkar, A. R., and As-Sawwaf, M. W., 1981, Seismicity studies in Saudi Arabia--Microearthquakes in the Jiddah area: Directorate General of Mineral Resources, Open-File Report DGMR-OF-01-08, 64 p.

Ministry of Defence, Director of Military Survey, United Kingdom, 1980, Political map of the Arabian Peninsula: U.S. Geological Survey and the Arabian American Oil Company, compilers, under sponsorship of the Kingdom of Saudi Arabia, Ministry of Petroleum and Mineral Resources and the U.S. Department of State, scale 1:2,250,000.

Mohr, P. A., 1975, Structural setting and evolution of Afar, in Pilger, A., and Rösler, A., eds., Afar depression of Ethiopia: Inter-Union Commission on Geodynamics, Scientific Report 14, Verlagsbuchhandlung, Stuttgart, p. 27-37.

Molnar, P., and Oliver, J., 1969, Lateral variations of attenuation in the upper mantle and discontinuities in the lithosphere: Journal of Geophysical Research, v. 74, p. 2648-2681.

Mooney, W. D., Gettings, M. E., Blank, H. R., and Healy, J. H., 1985, Saudi Arabian seismic deep-refraction profile--A travel time interpretation of deep crustal structure: Tectonophysics, v. 111, p. 173-246.

Morton, W. H., and Black, R., 1975, Crustal attenuation in Afar, in Pilger, A., and Rösler, A., eds., Afar depression of Ethiopia: Inter-Union Commission on Geodynamics, Scientific Report 14, Verlagsbuchhandlung, Stuttgart, p. 55-65.

Muller, E., Fredrich, K., and Klinge, H., 1984, Hydrogeology of the Tihamat Asir, in Jado, A. R., and Zitl, J. G., Quaternary Period in Saudi Arabia, V.Z.: New York, Springer-Verlag Publishers, p. 174-194.

Nishenko, S. P., and McCann, W. R., 1981, Seismic potential for the world's major plate boundaries, in Simpson, D. W., and Richards, P. G., eds, Earthquake prediction, an international review, Maurice Ewing series: American Geophysical Union, v. 4, p. 20-28.

Nuttli, O. W., 1983, Average seismic source-parameter relations for mid-plate earthquakes: Seismological Society of America Bulletin, v. 73, p. 519-535.

Nuttli, O. W., and Herrmann, R. B., 1984, Ground motion of Mississippi Valley earthquakes: Journal of Technical Topics in Civil Engineering, v. 110, p. 54-69.

Oaks, S. D., and Algermissen, S. T., 1984, Investigation of historical seismicity in the Salt Lake City portion of the Wasatch front region of Utah using documentary sources, in Hays, W. W., and Gori, P. L., eds., Proceedings of Conference XXVI, A workshop on evaluation of regional and urban earthquake hazards and risk in Utah: U.S. Geological Survey Open-File Report 84-763, p. 384-390.

Oliver, J., and Isacks, B., 1967, Deep earthquake zones, anomalous structures in the upper mantle, and the lithosphere: Journal of Geophysical Research, v. 72, p. 4259-4275.

Pallister, J. S., 1982, Reconnaissance geologic map of the Shu Ayba quadrangle, sheet 20/39, Kingdom of Saudi Arabia: Saudi Arabian Deputy Ministry for Mineral Resources Open-File Report USGS-OF-02-59, 1 pl. (Unpublished data)

_____, Explanatory notes to the geologic map of the Al Lith quadrangle, sheet 20 D, Kingdom of Saudi Arabia: Saudi Arabian Deputy Ministry for Mineral Resources Open-File Report USGS-OF-04-8, 124 p., 1 pl. (in press)

Phillips, J. D., and Ross, D. A., 1970, Continuous seismic reflexion profiles in the Red Sea: Philosophical Transactions of the Royal Society of London, v. 267, p. 143-152.

Pilger, A., and Risler, A., 1975, eds., Afar depression of Ethiopia: Inter-Union Commission on Geodynamics, Scientific Report 14, Verlagsbuchhandlung, Stuttgart, 416 p.

Poirier, J. P., and Taher, M. A., 1980, Historical seismicity in the Near and Middle East, North Africa, and Spain from Arabic documents (VIIth-XVIIth century): Seismological Society of America Bulletin, v. 70, no. 6, p. 2185-2201.

Project Rose Scientists, 1981, Microearthquake activity on the Orozco fracture zone--Preliminary results from project Rose: Journal of Geophysical Research, v. 86, p. 3783-3790.

Quennell, A. M., 1959, Tectonics of the Dead Sea rift: International Geology Congress, 20th, Mexico-Association Serv. Geol. Afr., p. 385-405.

Reches, Ze'ev, and Hoexter, D. F., 1981, Holocene seismic and tectonic activity in the Dead Sea area, in Freund, R., ed., The Dead Sea Rift-- International Symposium on the Dead Sea Rift, Jerusalem, Sept. 10-20, 1979--International Symposium on the Dead Sea Rift, Jerusalem, Sept. 10- 20, 1979: Tectonophysics, v. 80, p. 235-254.

Riad, S., 1977, Shear zones in North Egypt interpreted from gravity data: Geophysics, v. 42, no. 6, p. 1207-1214.

Ross, D. A., and Schlee, J., 1973, Shallow structure and geologic development in the southern Red Sea: Geological Society of America Bulletin, v. 84, p. 3827-3848.

_____1977, Shallow structures and geologic development of the southern Red Sea, in Red Sea research 1970-1975: Saudi Arabian Directorate General of Mineral Resources Bulletin 22, p. E1-E18.

Rowlett, H., 1981, Seismicity at intersections of spreading centers and transform faults: Journal of Geophysical Research, v. 86, p. 3815-3820.

Said, R., 1962, The geology of Egypt: New York, Elsevier, 377 p.

Schmidt, D. L., Hadley, D. G., and Brown, G. F., 1983, Middle Tertiary continental rift and evolution of the Red Sea in southwest Saudi Arabia, U.S. Geological Survey Open-File Report 83-641, 56 p.

Sieh, K. E., 1978, Prehistoric large earthquakes produced by slip on the San Andreas fault at Pallett Creek, California: Journal of Geophysical Research, v. 83, p. 3907-3939.

_____1981, A review of geological evidence for recurrence times of large earthquakes, in Simpson, D. W., and Richards, P. G., eds., Earthquake prediction, an International review, Maurice Ewing series: American Geophysical Union, v. 4, p. 181-207.

Solomon, S. C., 1973, Shear wave attenuation and melting beneath the mid-Atlantic ridge: Journal of Geophysical Research, v. 78, p. 6044-6059.

Solomon, S. C., and Burr, N. C., 1979, The relationship of source parameters of ridge-crest and transform earthquakes to the thermal structure of oceanic lithosphere: Tectonophysics, v. 55, p. 107-126.

Steinbrugge, K. V., 1984, Effects of shaking on buildings by class of construction, in Williams, M. E., ed., Proceedings of the Geologic and Hydrologic Hazards Training Program: U.S. Geological Survey Open-File Report 84- 760, p. 153-209.

Stepp, J. C., 1973, Analysis of completeness of the earthquake sample in the Puget Sound area, in Harding, S. T., ed., Contributions to Seismic Zoning: National Oceanic and Atmospheric Administration Technical Report ERL267-ESL30, p. 16-28.

Stewart, L. M., 1983, Strain release along oceanic transforms, Yale University, Ph.D. dissertation, 272 p.

Sykes, L. R., 1967, Mechanism of earthquakes and nature of faulting on the mid-ocean ridges: Journal of Geophysical Research, v. 72, p. 2131-2153.

_____1970, Focal mechanisms for earthquakes along the world rift system: Seismological Society of America Bulletin, v. 60, no. 5, p. 1749-1752.

_____1978, Intraplate seismicity reactivation of preexisting zones of weakness, alkaline magmatism, and other tectonism postdating continental fragmentation: Reviews of Geophysics and Space Physics, no. 4, p. 621-668.

Sykes, L. R., and Landisman, M., 1964, The seismicity of East Africa, the Gulf of Aden and the Arabian and Red Seas: Seismological Society of America Bulletin, v. 54, no. 6, p. 1927-1940.

Sykes, L. R., and Nishenko, S. P., 1984, Probabilities of occurrence of large plate rupturing earthquakes for the San Andreas, San Jacinto, and Imperial faults, California, 1983-2003: Journal of Geophysical Research, v. 89, p. 5905-5927.

Sykes, L. R., and Seeber, L., 1982, Great earthquakes and great asperities along the San Andreas fault, southern California [abs.]: EOS, Transactions of the American Geophysical Union, v. 63, p 1030.

Trehu, A. M., Nabelek, J. L., and Solomon, S. Ci, 1981, Source characterization of two Reykjanes Ridge earthquakes--Surface waves and moment tensors; P waveforms and nonorthogonal nodal planes: Journal of Geophysical Research, v. 86, p. 1701-1724.

Weichert, D. H., 1980, Estimation of earthquake recurrence parameters for unequal observation periods for different magnitudes: Seismological Society of America Bulletin, v. 70, p. 1337-1346.

Whitney, J. W., 1982, Overview of the geomorphology of western Saudi Arabia and recommendations for future research: Saudi Arabian Deputy Ministry for Mineral Resources Open-File Report USGS-OF-02-6, 19 p. (Unpublished data)

Wilson, J. T., 1965, A new class of faults and their bearing on continental drift: Nature, v. 207, p. 343-347.

Youd, T. L., 1984, Geologic effects-liquefaction and associated ground failure, in Williams, M. E., Proceedings of the Geologic and Hydrologic Hazards Training Program' U.S. Geological Survey Open-File Report 84- 760, p. 210-232.

Youd, T. L., and Perkins, D. M., 1978, Mapping of liquefaction-induced ground failure potential: American Society of Civil Engineers, Journal of the Geotechnical Engineering Division, v. 104, no. GT4, p. 433-466.

Zanettin, B., and Justin-Visentin, E., 1975, Tectonical and volcanological evolution of the western Afar margin (Ethiopia), in Pilger, A., and Risler, A., eds., Afar Depression of Ethiopia: Inter-Union Commission on Geodynamics, Scientific Report No. 14, Verlagsbuchhandlund, Stuttgart, p. 300-309.